



University of
Stavanger

Faculty of Science and Technology

MASTER'S THESIS

| | |
|---|--|
| Study program/ Specialization: Petroleum technology | Spring semester, 2013 Open access |
| Writer: Silje Ramvik | (<u>W</u> riter's signature) |
| Faculty supervisor: Helge Hodne | |
| Title of thesis: Application of fly ash-based geopolymer as an alternative material for plug and abandonment | |
| Credits (ECTS): 30 | |
| Key words: Plugging and abandonment Portland cement and additives Geopolymers Fly ash Ultrasonic Cement Analyzer Uniaxial Compressive Strength test | Pages: 88 Stavanger, 30/05/2013 |

Acknowledgements

This thesis is a supplement to Mahmoud Khalifeh's work on his PhD regarding geopolymers. The work with this thesis was performed at the University of Stavanger (UiS). The laboratory work was performed at the cement lab at UiS.

I would especially like to thank my supervisor at UiS, Helge Hodne, for introducing me to the field of geopolymers, for shearing this knowledge and insight, and for providing feedback regarding the work. I would also like to thank Helge for the help and guidance during the laboratory experiments.

Also, I would like to thank Mahmoud Khalifeh for providing inspiration and guidance during the work with this thesis, as well as helping me during the laboratory experiments.

Abstract

In this study fly ash-based geopolymers were produced by the alkali-activation of fly ash. The purpose was to use fly ash-based geopolymers as alternative for cement for plug and abandonment operations. Ultrasonic Cement Analyzers (UCAs) were used to investigate the instantaneous strength development and Uniaxial Compressive Strength tests were performed to compare the results with the UCA results.

Several different recipes were made for the UCA tests and the compressive strength development for each recipe was measured. Adjustments were made to the recipe after each experiment to optimize the ingredients and increase the maximum compressive strength. When the final recipe was found, the obtained result from the UCA was tested in several UCS tests. During the experiments several different materials were used. However, it was found from the UCA results that the recipe containing only fly ash and alkali activators gave the best results; a continuous positive trend in the compressive strength development. The UCS tests showed higher compressive strength for the same recipe, indicating that the recipe had promising properties. During the UCS tests it was also found that a higher concentration of sodium hydroxide resulted in higher compressive strength.

The results found in these experiments indicate that there is a potential to use fly ash-based geopolymers as an alternative cementing material for plug and abandonment. However, there is a need for further research on the subject before the geopolymers can be used in practice.

Table of Contents

| | |
|--|------------|
| Acknowledgements | I |
| Abstract | III |
| List of figures | VII |
| List of tables | X |
| Nomenclature | XI |
| 1. Introduction | 1 |
| 2. Objective | 3 |
| 3. Plug and abandonment | 4 |
| 3.1. Barriers | 4 |
| 3.2. Barrier positioning requirements..... | 4 |
| 3.3. Temporary plug and abandonment requirements | 6 |
| 3.4. Permanent plug and abandonment requirements | 6 |
| 3.5. Verification requirements of a cement plug | 7 |
| 4. Setting a permanent plug | 8 |
| 4.1. Placement of a permanent plug..... | 8 |
| 4.2. Plug placement techniques | 9 |
| 4.2.1. <i>The balanced plug method</i> | 9 |
| 4.2.2. <i>The dump bailer method</i> | 10 |
| 4.2.3. <i>The two-plug method</i> | 11 |
| 4.3. New technologies..... | 12 |
| 5. Plugging materials | 13 |
| 5.1. Plugging material requirements..... | 13 |
| 5.2. Portland cement..... | 15 |
| 5.2.1. <i>Manufacturing Portland cement</i> | 15 |
| 5.2.2. <i>Portland cement materials</i> | 18 |
| 5.2.3. <i>Cement additives</i> | 20 |
| 5.3. Geopolymers | 24 |
| 5.3.1. <i>Raw materials for geopolymers</i> | 24 |
| 5.3.2. <i>Manufacturing geopolymers</i> | 25 |
| 5.3.3. <i>Geopolymers properties</i> | 26 |
| 6. Experimental conditions | 27 |

| | | |
|-----------|---|-----------|
| 6.1. | Materials..... | 27 |
| 6.1.1. | <i>Fly ash</i> | 27 |
| 6.1.2. | <i>Blast Furnace Slag</i> | 28 |
| 6.1.3. | <i>Metakaolin</i> | 29 |
| 6.1.4. | <i>Water glass</i> | 29 |
| 6.1.5. | <i>Silicon dioxide</i> | 30 |
| 6.1.6. | <i>Micro silica</i> | 30 |
| 6.1.7. | <i>Sodium hydroxide</i> | 31 |
| 6.2. | Equipment | 32 |
| 6.2.1. | <i>Ultrasonic Cement Analyzer</i> | 32 |
| 6.2.2. | <i>Uniaxial Compressive Strength</i> | 33 |
| 6.3. | Mixing procedure | 34 |
| 6.4. | Test results | 35 |
| 6.4.1. | <i>Ultrasonic Cement Analyzer test</i> | 35 |
| 6.4.2. | <i>Uniaxial Compressive Strength tests</i> | 43 |
| 6.5. | Discussion..... | 49 |
| 6.5.1. | <i>Comparison of the Ultrasonic Cement Analyzer results</i> | 49 |
| 6.5.2. | <i>Comparison of the UCA and UCS results</i> | 54 |
| 6.6. | Proposed further work | 55 |
| 6.7. | Conclusion | 56 |
| 7. | References | 57 |
| | Appendix A | 60 |
| | Appendix B | 67 |

List of figures

| | |
|--|----|
| Figure 3.1: Schematics of the general barrier requirements for well abandonment (from Oil & Gas UK guidelines (2012)) [8]..... | 5 |
| Figure 4.1: Schematics of the balanced plug method (from Nelson and Guillot (2006)) [11]. | 9 |
| Figure 4.2: Schematics of the dump bailer method (from Nelson and Guillot (2006)) [11]. | 10 |
| Figure 4.3: Schematics of the two-plug method (from Nelson and Guillot (2006)) [11]. | 11 |
| Figure 5.1: Schematic flow diagram of the dry calcination process (from Nelson and Guillot (2006)) [11]..... | 16 |
| Figure 5.2: Schematic flow diagram of the wet calcination process (from Nelson and Guillot (2006)) [11]..... | 16 |
| Figure 5.3: Schematic flow diagram of the burning process (from Nelson and Guillot (2006)) [11]. | 17 |
| Figure 6.1: Ultrasonic Cement Analyzer (UCA) system..... | 32 |
| Figure 6.2: Pressure controller connected to the UCA system.. | 32 |
| Figure 6.3: Graphical presentation of the result from the UCA test of sample no. 58. Performed at a curing pressure of 5100 psi and curing temperature of 88°C. | 36 |
| Figure 6.4: Graphical presentation of the result from the UCA test of sample no. 62. Performed at a curing pressure of 5100 psi and curing temperature of 88°C. | 37 |
| Figure 6.5: Graphical presentation of the result from the UCA test of sample no. 76. Performed at a curing pressure of 5100 psi and curing temperature of 88°C. | 38 |
| Figure 6.6: Graphical presentation of the result from the UCA test of sample no. 84. Performed at a curing pressure of 5100 psi and curing temperature of 88°C. | 39 |
| Figure 6.7: Graphical presentation of the result from the UCA test of sample no. 87. Performed at a curing pressure of 5100 psi and curing temperature of 88°C. | 40 |
| Figure 6.8: Graphical presentation of the result from the UCA test of sample no. 100. Performed at a curing pressure of 5100 psi and curing temperature of 88°C. | 41 |
| Figure 6.9: Graphical presentation of the result from the UCA test of sample no. 130. Performed at a curing pressure of 5100 psi and curing temperature of 88°C. | 42 |
| Figure 6.10: Sample no. 115 D showing a clear crack throughout the sample | 45 |
| Figure 6.11: SEM image of sample 115 B with a magnitude of 1000. Showing circular particles which are fly ash particles that have not reacted with the alkali solution. | 46 |
| Figure 6.12: SEM image of sample 115 B with a magnitude of 10 000. Showing an amorphous area of the sample. | 47 |
| Figure 6.13: SEM image of sample 115 B with a magnitude of 50 000. Showing an unspecified area of the sample. | 47 |

| | |
|---|----|
| Figure 6.14: Figure illustrates the effect of removing MK-750 content in no. 62 on the compressive strength. Performed at a curing pressure of 5100 psi and curing temperature of 88°C. | 49 |
| Figure 6.15: Figure illustrates the effect of increased amount of MK-750, water glass and 8M NaOH in no. 76. Performed at curing pressure of 5100 psi and curing temperature of 88°C..... | 50 |
| Figure 6.16: Figure illustrated the effect of increased amount of MK-750, 8M NaOH and water glass and decreased amount of silica in no. 87. Performed at curing pressure of 5100 psi and curing temperature of 88°C. | 51 |
| Figure 6.17: Figure illustrates the effect of increased amount of 8M NaOH and decreased amount of water glass content in no. 100. Performed at a curing pressure of 5100 psi and a curing temperature of 88°C. | 52 |
| Figure 6.18: Figure illustrates the effect of removing MK-750, silica and BFS in no. 130. Performed at a curing pressure of 5100 psi and a curing temperature of 88°C. | 53 |
| Figure A.1: UCA results for test no. 58. The upper blue curve shows the transit time (micro sec/in), the middle green curve shows the compressive strength (psi) and the lower red curve shows the temperature (°C). | 60 |
| Figure A.2: UCA results for test no. 62. The upper blue curve shows the transit time (micro sec/in), the middle green curve shows the compressive strength (psi) and the lower constant red curve shows the temperature (°C). | 61 |
| Figure A.3: UCA results for test no. 76. The upper blue curve shows the transit time (micro sec/in), the middle green curve shows the compressive strength (psi) and the lower red curve shows the temperature (°C). | 62 |
| Figure A.4: UCA results for test no. 84. The upper blue curve shows the transit time (micro sec/in), the middle green curve shows the compressive strength (psi) and the lower red curve shows the temperature (°C). | 63 |
| Figure A.5: UCA results for test no. 87. The upper blue curve shows the transit time (micro sec/in), the middle red curve shows the temperature (°C) and the lower green curve shows the compressive strength (psi). | 64 |
| Figure A.6: UCA results for test no. 100. The upper blue curve shows the transit time (micro sec/in), the constant middle red curve shows the temperature (°C) and the lower green curve (crossing the middle red curve at one point) shows the compressive strength (psi)..... | 65 |
| Figure A.7: UCA results for test no. 130. The upper blue curve shows the transit time (micro sec/in), the middle green curve shows the compressive strength (psi) and the lower red curve shows the temperature (°C). | 66 |

| | |
|---|----|
| Figure B.1: Results and graph for sample 115 A from the UCS test. The graph shows the applied force (kN) on the y-axis and the time (sec) on the x-axis. | 67 |
| Figure B.2: Results and graph for sample 115 B from the UCS test. The graph shows the applied force (kN) on the y-axis and the time (sec) on the x-axis. | 68 |
| Figure B.3: Results and graph for sample 115 C from the UCS test. The graph shows the applied force (kN) on the y-axis and the time (sec) on the x-axis. | 69 |
| Figure B.4: Results and graph for sample 131 A from the UCS test. The graph shows the applied force (kN) on the y-axis and the time (sec) on the x-axis. | 70 |
| Figure B.5: Results and graph for sample 131 B from the UCS test. The graph shows the applied force (kN) on the y-axis and the time (sec) on the x-axis. | 71 |
| Figure B.6: Results and graph for sample 132 A from the UCS test. The graph shows the applied force (kN) on the y-axis and the time (sec) on the x-axis. | 72 |
| Figure B.7: Results and graph for sample 132 B from the UCS test. The graph shows the applied force (kN) on the y-axis and the time (sec) on the x-axis. | 73 |

List of tables

| | |
|---|----|
| Table 5.1: List of material types for permanent barriers (from the Oil & Gas UK guidelines (2012)) [9]. | 14 |
| Table 5.2: Various raw materials used in producing clinker for Portland cement (from Nelson and Guillot (2006)) [11]. | 19 |
| Table 5.3: Composition, cement notation and concentration of minerals in Portland cement (from Nelson and Guillot (2006)) [11]. | 20 |
| Table 6.1: Chemical requirements for fly ashes (from Nelson and Guillot (2006)) [11]. | 28 |
| Table 6.2: Composition of micro silica delivered by Elkem (Norway). | 31 |
| Table 6.3: Recipes and solid-liquid ratio of the samples. | 35 |
| Table 6.4: Key features from the original graph are tabulated in Appendix A, for test no. 58. | 36 |
| Table 6.5: Key features from the original graph are tabulated in Appendix A, for test no. 62. | 37 |
| Table 6.6: Key features from the original graph are tabulated in Appendix A, for test no. 76. | 38 |
| Table 6.7: Key features from the original graph are tabulated in Appendix A, for test no. 84. | 39 |
| Table 6.8: Key features from the original graph are tabulated in Appendix A, for test no. 87. | 40 |
| Table 6.9: Key features from the original graph are tabulated in Appendix A, for test no. 100. | 41 |
| Table 6.10: Key features from the original graph are tabulated in Appendix A, for test no. 130. | 42 |
| Table 6.11: Recipes of sample 115 A-G. | 43 |
| Table 6.12: Recipes of sample 131 A and B. | 44 |
| Table 6.13: Recipes of sample 132 A and B. | 44 |
| Table 6.14: Results for test no. 115 A-G from the UCS tests. | 45 |
| Table 6.15: Results for test no. 131 A and B from the UCS test. | 48 |
| Table 6.16: Results for test no. 132 A and B from the UCS test. | 48 |
| Table 6.17: Results from the UCS tests. | 54 |

Nomenclature

| | | |
|--------------------------------|---|---|
| Al ₂ O ₃ | - | Aluminum oxide |
| ASTM | - | American Society for Testing and Minerals |
| BFS | - | Blast-furnace slag |
| CaO | - | Calcium oxide |
| CO ₂ | - | Carbon dioxide |
| C ₂ S | - | Belite |
| C ₃ A | - | Aluminate |
| C ₃ S | - | Alite |
| C ₄ AF | - | Ferrite phase |
| DHSV | - | Downhole Safety Valve |
| Fe ₂ O ₃ | - | Iron oxide |
| g/cm ³ | - | Gram per cubic meter |
| H ₂ S | - | Hydrogen sulphide |
| kN | - | kilo Newton |
| M | - | Molar |
| MD | - | Measured depth |
| MK-750 | - | Metakaolin |
| ms/in | - | micro second/inch |
| NaCl | - | Sodium chloride |
| NaOH | - | Sodium hydroxide |
| Na ₂ O | - | Sodium oxide |
| NCS | - | Norwegian Continental Shelf |
| No. | - | Number |
| N/A | - | Not available |
| Oil & Gas UK | - | Oil & Gas United Kingdom |
| PSA | - | Petroleum Safety Authority Norway |
| P&A | - | Plug and Abandonment |
| PWC | - | Perforate, Wash and Cement |
| SEM | - | Scanning Electron Microscope |
| SiO ₂ | - | Silicon dioxide (silica) |
| SLR | - | Solid-liquid ratio |
| UCA | - | Ultrasonic Cement Analyzer |
| UCS | - | Uniaxial Compressive Strength |
| UiS | - | University of Stavanger |
| U.S. | - | United States of America |
| WBE | - | Well Barrier Element |
| µm | - | Micrometer |

1.Introduction

During the last century there have been drilled several million wells worldwide for various reasons like industrial applications, disposal/injection, oil and gas, testing/seismic or exploration [1]. During these wells` life cycle some will fail and some will wear out or no longer have an economically efficient production. When wells reach this stage they are abandoned. Abandonment involves setting barriers to isolate the different zones from each other. The barriers that are set may either be temporary, to be able to re-enter the well, or permanent. One of the main reasons for performing plug and abandonment (P&A) is to prevent contamination of fresh water and nearby formations.

Early in the 1900s there did not exist any regulations in the United States (U.S.) stating how a well had be plugged when it was abandoned to ensure a proper sealing [1]. This resulted in several poorly plugged wells, high plug failure rate and in some places the ground waters were contaminated due to nearby wells. The contamination was the consequence of cross-flow, meaning that fluid flows from one subsurface formation to another. Since more than half of the U.S. uses ground waters as their main water supply, the regulations had to be changed.

In the 1930s laws and oil and gas agencies like the Interstate Oil Compact Commission (now known as the Interstate Oil and Gas Compact Commission) were established. In 1956 the Oil, Gas and Coal Mining Act was introduced. The Oil, Gas and Coal Mining Act stated that all drilled oil and gas wells were to be put on record upon completion. Regulations in the U.S. today requires that before drilling is allowed, a form explaining the purpose of the well and a plan for P&A must be submitted [1]. The regulations also require that the placement of the plug has to isolate productive-, water- and pressurized zones and that the plugging material has to be impermeable and long lasting. In some states in the U.S. the regulations also require that the plug has to be tagged and tested to ensure proper sealing after a P&A operation, before it is approved.

The issue about the drinking water, as in the U.S., is not a concern on the Norwegian Continental Shelf (NCS), but avoiding cross-flow is still important. When drilling wells close to each other, as on the NCS, the importance of maintaining the reservoir pressure is major to be able to transport oil and gas to the surface [2]. Even though a well is being abandoned, nearby wells that are producing should not be affected by losing its reservoir pressure. On the NCS the regulations for permanently plugging a well is governed by the Petroleum Safety Authority Norway (PSA) and NORSOK D-010 is the standard that has to be used as minimum functional requirement for well operations in Norway [3], [4]. Other standards

may also be used; as long as it can be proved that the standard is equally good or better than the NORSOK D-010 requirements.

Since the first hydrocarbon well was drilled on the NCS in 1966, there have been drilled 3800 wells [5]. 800 of these wells have been temporary abandoned and 170 wells have been permanently abandoned. Because P&A is a fairly new technology there are still uncertainties concerning the operating and the plugging materials that are used. So, in 2006, PSA performed a “pilot well integrity survey” on 406 wells from seven operating companies [6]. Well integrity includes a wells whole life cycle, from design to final stage: P&A. The wells differed in both age and development categories to get a varied perspective of the wells integrity, but no wells with P&A were studied. However, the selection of wells does give insight into the general well integrity status of NCS wells. According to the project 18% of the wells had integrity failures, while 7% of these were shut down due to well integrity issues. Most of the problems found were related to the downhole safety valve (DHSV) and tubing leaks of wells from the early 1900s, but these failures are not relevant in P&A since the DHSV and tubing are removed before an P&A operation. However, 8 wells with failed cement as a well barrier element (WBE) were found, and all of these wells were less than 14 years old when the survey was conducted. The cement failures indicate that cement problems may continue to occur in the future, causing problems in P&A wells. This gives an opportunity to improve the P&A technology by developing a new and more resistant plugging material.

2. Objective

Geopolymers is a developing field of research for replacing the most widely used plugging material in plug and abandonment; Portland cement. Fly ash-based geopolymers was studied as an alternative in this thesis. Fly ash-based geopolymers were produced by the alkali-activation of fly ash with an activator solution. Several different additives were also added in the recipes. The objective of this thesis was to analyze the compressive strength buildup of fly as-based geopolymers under high pressure and high temperature conditions and thereby find a recipe that was able to build enough strength to compete with Portland cement.

To analyze the compressive strength of the geopolymers samples an Ultrasonic Cement Analyzer (UCA) was used. If the preferred compressive strength was not achieved, there was made an adjustment to the recipe to optimize it. This was repeated several times to increase the compressive strength until the desired values were reached. When the preferred compressive strength buildup was achieved, the results were verified using Uniaxial Compressive Strength (UCS) tests.

3. Plug and abandonment

According to the Oil & Gas UK guideline on well abandonment cost estimation (2011) a P&A operation can be divided into three phases [7]. These are; reservoir abandonment, intermediate abandonment and wellhead and conductor removal. These phases reflect the work-scope, equipment required, and the discrete timing of the different phases of the work. The first phase involves setting the primary and secondary permanent barriers that fully isolates the reservoir from the wellbore. The second phase involves isolating liners, milling and retrieving casings. It also includes setting the shallower barriers and surface barrier. The third phase involves retrieving the well head, the conductor and fill the craters with cement. In this thesis the issues regarding P&A will be presented, hence, removal of casing and well head will not be discussed. In the next sections barriers and requirements regarding P&A will be presented.

3.1. Barriers

In NORSOK D-010 a well barrier is defined as [4]:

“an envelope of one or several dependent WBEs (Well Barrier Elements) preventing fluids or gases from flowing unintentionally from a formation into another formation or to surface” [4].

A well is required to have two verified well barriers in case of increased pore pressure that may lead to uncontrolled flow from the reservoir [4]. These well barriers should be independent and not have common well barrier elements (WBE). However, in some cases a common WBE may be accepted after doing a risk analysis and reducing the risk to as low as reasonably practicable, and testing the WBEs in the relevant flow directions. The WBEs can be designed to either seal in one or both directions. When the purpose is to seal in one direction an inflow test can be performed. This implies reducing the pressure on the downstream side of the barrier to a minimum. Otherwise, if the purpose is to seal in both directions, the WBE can be tested against flow. One of the most important requirements regarding the WBEs is that if one WBE fail, this cannot lead to uncontrolled flow from the wellbore.

3.2. Barrier positioning requirements

According to the Oil & Gas United Kingdom (Oil & Gas UK) Guidelines for the Suspension and Abandonment of Wells, released in July 2012, the two barriers should be located as follows [8]:

The first barrier should be set as close as reasonably possible to the inflow source. If the barrier is to be set inside a liner or casing, it should be overlain by annular cement. In the cases where the barrier is set above the inflow point, the fracture pressure at the base of the barrier should be higher than the

potential internal pressure that may be present. The second barrier should first of all backup the first barrier, meaning that the second barrier must be placed in such a way that the formation fracture pressure at the base is higher than the potential internal pressure that may be present. Note that the second barrier may be used as the first barrier for another, shallower positioned, permeable zone.

NORSOK D-010 also requires that the firm plug must be located at a minimum of 100 meters measured depth (MD) to ensure that the plug seals off the whole cross section [4]. When a mechanical plug is used as foundation inside a casing, a minimum of 50 meters MD is required. The cement must as well extend to 50 meters above the source of inflow or above the last casing shoe when the plug is in transition from open hole to casing.

Fig. 3.1 borrowed from the Oil & Gas UK guideline on well abandonment cost estimation (2012), illustrates a schematic of the general requirements for abandonment, including both first and secondary barriers for zone A and B [8]. It should however be mentioned that abandonment schematics may be different for each well, since no well has the same conditions.

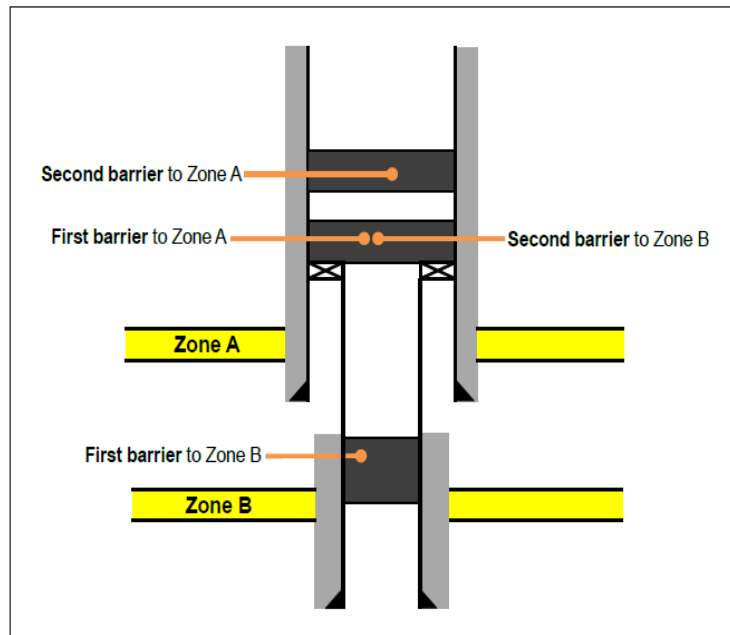


Figure 3.1: Schematics of the general barrier requirements for well abandonment (from Oil & Gas UK guidelines (2012)) [8].

3.3. Temporary plug and abandonment requirements

NORSOK D-010 requires that it have to be possible to re-enter a temporarily abandoned well at a later stage in a safe manner [4]. The integrity of the materials that is used in a temporary abandoned well must withstand to at least two times its planned period of abandonment. In some cases a mechanical well barrier may be accepted, based on the planned abandonment period and subsurface environment.

3.4. Permanent plug and abandonment requirements

When it comes to permanent P&A the requirement of two well barriers is not sufficient anymore [4]. For permanent P&A there are requirements for an open hole surface well barrier and a well barrier between reservoirs in addition to the primary and secondary barrier. The open hole barrier isolates and acts as a final barrier against flow from the hole to the surface after the casing has been cut, while the well barrier between the reservoirs isolates the different zones from each other. As for the Oil & Gas UK guidelines, NORSOK also requires the position of the well barrier to be set as close to the potential source of inflow as possible and where the formation fracture pressure is estimated to be larger than the inside pressure.

According to the requirements in NORSOK D-010 a permanent well barrier must extend to the full cross section of the well, include all annuli as well as seal in both horizontal and vertical directions [4]. Hence, a WBE set inside the casing must be placed where there is verified cement present in the annulus or an equivalent WBE. When setting the plug it is crucial that there is no fluid movement after the cement is set and before it has built adequate strength [1]. If this requirement is not fulfilled the plug may become soft and fail.

According to NORSOK D-010 a permanent well barrier should have the following properties [4]:

- 1) *“Impermeable*
- 2) *Long term integrity.*
- 3) *Non-shrinking.*
- 4) *Ductile – (non-brittle) – able to withstand mechanical loads/impact.*
- 5) *Resistance to different chemicals/ substances (H₂S, CO₂ and hydrocarbons).*
- 6) *Wetting, to ensure bonding to steel.” [4]*

After placement, the barrier material must be able to withstand vibrations, the surrounding pressure and temperature and the external loadings [9]. The barriers must also be designed to withstand exposure to non-native chemicals and native substances such as hydrocarbons, CO₂, H₂S and brine, as well as handling contact with water (no unwanted swelling).

To be allowed to perform a permanent P&A, Norsok D-010 defines several requirements regarding the design basis and which information that needs to be collected, as a minimum [4]. Norsok D-010 states that when using cement for abandonment the design basis should take into account uncertainties regarding:

- *“downhole placement techniques*
- *minimum volumes required to mix a homogenous slurry,*
- *surface volume control, pump efficiency/ -parameters,*
- *contamination of fluids,*
- *shrinkage of cement.” [4]*

Norsok D-010 also recommends gathering some other data, such as depth of the well, information about the permeable formations, the wells production potential and information regarding primary cementing operations [4]. However, these data are not required. When all the data is gathered and the operation plan meets the Norsok requirements, the plugging operation can begin.

3.5. Verification requirements of a cement plug

Norsok D-010 describes several requirements regarding verification of the cement plug. First of all the strength of the plug must be pre-tested before being used [4]. A pre-test involves using the same kind of tools, cement and fluids and simulating the wellbore and formation conditions to verify if the plug will meet all requirements. The simulation will not be entirely accurate, but as close as possible.

When the plug is set its position should be verified by means of tagging to confirm the depth of the plug [4]. Tagging is when a drill pipe or coiled tubing is lowered down into the hole until it touches the plug and a reduction in weight of tool is detected and thereby knowing the position of the plug. When the position is verified the strength of the plug must be checked [4]. This is done by performing a pressure test. Norsok D-010 describes the pressure test requirements as follows; the pressure during the test shall be 1000 psi above the estimated formation strength below the casing or 500 psi for surface casing plugs. During the pressure test the pressure cannot exceed the casing or cement strength. If the strength of the plug is approved, the verification operation is completed.

4. Setting a permanent plug

Cement plugs play an important part in many operations throughout the lifetime of the well, including lost circulation, zonal isolation, kick-off and abandonment. Setting a quality cement plug in a well that shall be abandoned is essential and is dependent on good job planning, taking the specific well conditions into account. Conventionally there are three main steps when setting a permanent plug; logging, milling and underreaming. Milling is the most time consuming operation and that is why there is a high focus on reducing the time used during milling. New technologies that may reduce the P&A operation time will be presented in the next sections as well as placement of a permanent plug and plug placement techniques.

4.1. Placement of a permanent plug

Before a plug can be set, the cement job behind the casing has to be checked [10]. A logging operation is carried out to verify the cement job. The most used logging method is acoustic logging [11]. The method is based on a tool that consists of several senders and receivers that transmits acoustic sound waves and records the travelling time of the waves. The record information can then be analyzed. Based on the knowledge that each material and fluid has different properties and thereby different travelling time, a prediction of how the cement behind the casing is can be made. If the cement behind the casing is sufficient, the plugging operation can begin immediately. However, if the cement job is not verified the cement needs to be removed. The operations that involve removing the cement and preparing the well for plugging can be divided into three stages; milling, clean-out run and underreaming run [10]. As mentioned earlier, it is the milling operation that is the most time consuming operation. Milling involves using cutters to cut the casing into metal debris that afterwards are being transported to the surface. To remove the metal debris there is a requirement for a swarf unit at the rig, which is undesirable in terms of the safety for the crew. According to NORSOK D-010 it is required that 50 meters of the casing have to be removed before setting a plug [4]. After the milling is completed, the clean-out run can begin. The clean-out run prepares the hole for cementing. When the clean-out run is completed, the underreaming run can start [10]. Underreaming is carried out to increase the hole diameter. This is done to remove any previously set cement and to expose new formation to allow better bonding and sealing properties for the new cement that shall be set. Finally, the plug can be set.

As mentioned, it is essential that there are no fluid movements in the hole where the plug has been set before the plug has built up strength [1]. To get an idea of how long it takes before the plug has set, lab tests on the relevant plug are often performed. This means that the formation conditions where the plug

shall be set can be simulated onshore. These conditions will not be totally accurate, but as close as possible, giving the operators an indication of how long it will take before the plug has built up strength and how long it takes before another operation can begin.

4.2. Plug placement techniques

There are several methods for setting a plug. In the next sections three of these methods will be explained briefly; the balanced plug method, the dump bailer method and the two-plug method, respectively.

4.2.1. The balanced plug method

The balanced method, illustrated in Fig. 4.1, is based on using a spacer fluid to separate the mud and cement slurry when pumping down cement [11]. A base, a bridge plug or a high viscous fluid, is used to set the plug in the right position in the well. Spacer, followed by cement slurry and spacer on top again, is pumped down the pipe onto the base, forcing the mud up the annulus. When the desired height of cement slurry is reached and there is equal height of cement slurry and spacer in both the pipe and the annulus, the pipe is slowly pulled out, allowing the cement slurry to solidify. This is a simple method that can be used with both drill pipes and coiled tubing and is therefore the most commonly used method. The main disadvantage using this method is the risk of mixing cement with other fluids such as drilling fluids or spacer, due to viscosity differences. The mixing of cement with other fluids may contaminate the cement and thereby prevent the cement to form a competent plug.

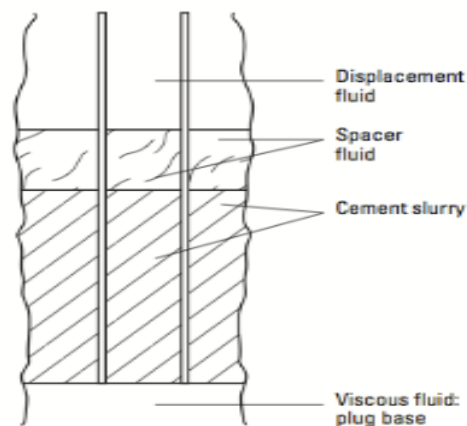


Figure 4.1: Schematics of the balanced plug method (from Nelson and Guillot (2006)) [11].

4.2.2. The dump bailer method

The dump bailer method is illustrated in Fig. 4.2. This method uses wire line to run down a dump bailer containing cement slurry into the wellbore [11]. The dump bailer method allows better control of where the cement slurry is placed. When the dump bailer is lowered down it touches a permanent bridge plug below the desired plug interval that opens the dump bailer using an electrical or a mechanical opening mechanism. Cement slurry is dumped upon the bridge plug while the dump bailer is pulled out of the wellbore.

The main advantage with using this method is that there is no need for a rig to do the operation, instead vessels can be used [11]. A disadvantage when using this method is due to the small volume of the dump bailer, it may be necessary to do several runs to obtain the wanted height of cement slurry, which is very time consuming. Another disadvantage may be that when pulling out the dump bailer the mud may swab into the dump bailer and contaminate it, requiring clean-outs before doing a second run.

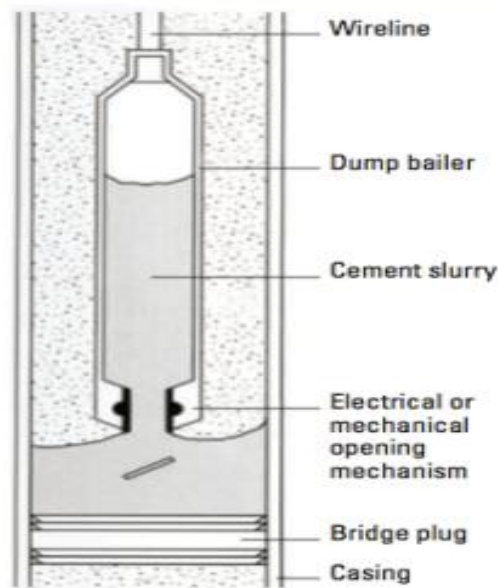


Figure 4.2: Schematics of the dump bailer method (from Nelson and Guillot (2006)) [11].

4.2.3. The two-plug method

The two-plug method, illustrated in Fig. 4.3, is based on using a special tool to set the plug at a calculated depth [11]. The tool consists of two wiper darts, a locator sub, a cement stinger and a diverter sub. The two wiper darts prevent fluids from mixing during the plug placement. The locator sub prevents the wiper darts from entering the bottom of the borehole and the cement stinger and the diverter sub guide the spacer and cement to the right position.

First spacer is pumped down, followed by the first wiper dart and cement on top. When the wiper dart reaches the locator sub, it stops, and the pressure above increases until a membrane in the wiper dart is broken, allowing cement to continue down the stinger. The cement is then followed by the second wiper dart with spacer on top. The second wiper dart stops and breaks at the locator sub, and the spacer is pumped further down. To prevent the spacer from going all the way down and mix with the cement, the stinger is pulled above the cement. The main challenge of this method is to pull the stinger up at the right time, to prevent the cement and spacer from mixing.

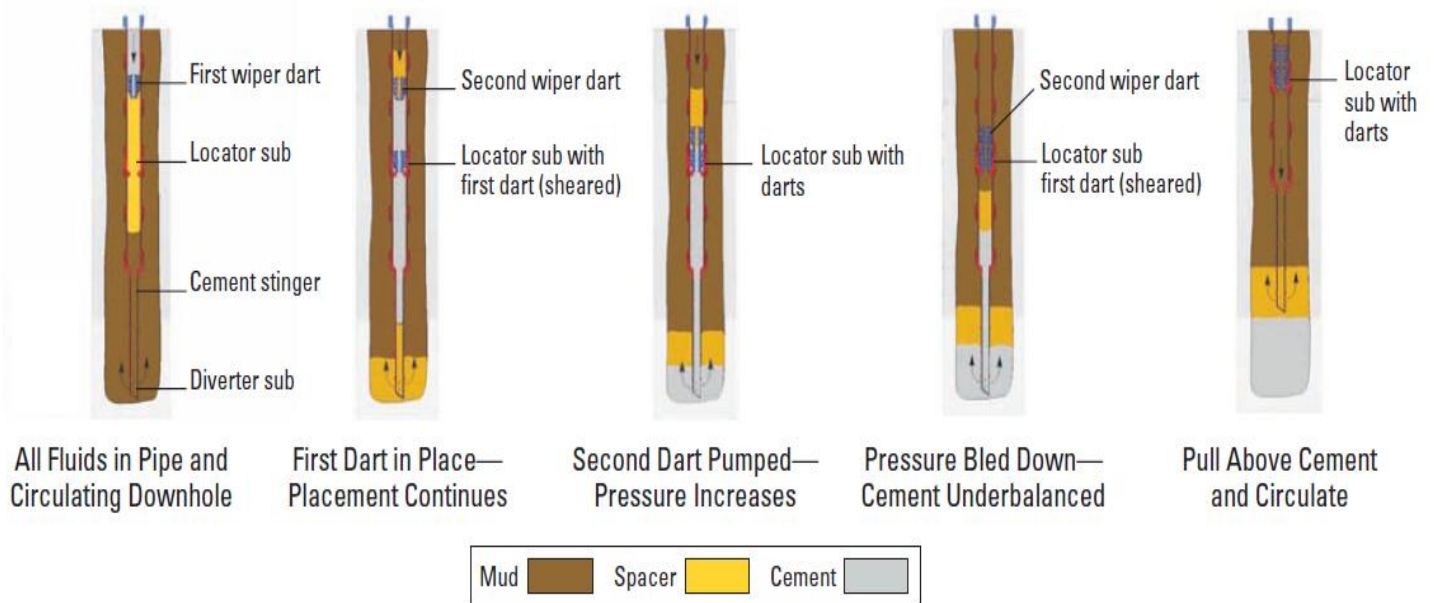


Figure 4.3: Schematics of the two-plug method (from Nelson and Guillot (2006)) [11].

4.3. New technologies

Since milling is the most time consuming operation there has been an increased focus on reducing the milling operation time. During a P&A campaign in 2008 on Ekofisk Whisky platform, Conoco Phillips completed two of eight P&A operations [10]. It was then found that the milling operation took, at an average, 65 days per well that was abandoned. So in 2009 Baker Hughes and Conoco Phillips introduced two new technologies that would reduce the time during milling operations. The two new technologies included a new cutter and a downhole optimization tool. The cutters had more resistant cutter materials which extended the lifetime of the cutters, allowing to mill larger sections without having to trip out and change milling tool. The downhole optimization tool sent real time data like weight on tool, torque, bending moment, vibrations, pressures and temperatures to the surface during milling. This gave the driller a better understanding of what went on in the hole as well as having the possibility to adjust the milling according to the downhole information during the operation. These two new technologies were used on the last six wells that were abandoned on the Ekofisk Whisky platform. The new technologies showed to reduce the operation time from 65 days to an average of 46 days.

A new system, the Perforate, Wash and Cement (PWC) system, has later on been proposed to reduce the operation time during P&A [10]. The PWC system makes it possible to perforate the uncemented casing, wash the hole and mechanically place the cement across the wellbore in one single run. The PWC system consists of a 50 meter drill pipe with guns that perforate the casing and drop the guns in a rat-hole afterwards. Meaning; the tool is left in the well bore. When the perforating guns are dropped, the wash tool is activated with balls that are dropped from the surface. Afterwards the wash tool is released using the same method. The released wash tool is then used as the base for the plug. The cementing tool is then activated and the borehole is cemented. The PWC system provides a good well control as well as reducing the surge and swab effects since there are no open perforations that can take or give fluid [10]. The main advantage is the large decrease in operation time and costs. Another advantage is that this system does not require a swarf unit, meaning that personnel are not exposed to swarf handling, reducing the potential injuries. In addition, there is no need for transport or disposals of metal debris. However, it has shown to be difficult to wash behind the casing as well as verifying the cement job behind the casing when using the PWC system.

5. Plugging materials

5.1. Plugging material requirements

In NORSOK D-010 a specification of plugging materials is not given, but instead, the functional requirements for the materials [4]. The standard does however mention some unacceptable materials for permanent well barriers:

“Steel tubular is not an acceptable permanent WBE unless it is supported by cement, or a plugging material with similar functional properties [...].

Elastomer seals used as sealing components in WBEs are not acceptable for permanent well barriers.”. [4]

The main cementing material is Portland cement, however the Oil & Gas UK Guidelines of qualification of materials for the suspension and abandonment of wells (2012) allows the use of alternative materials, and this is stated as follows [9]:

“Cement is currently used in wells as the prime material for abandonment purpose. This does not preclude the use of other materials. Alternative materials should, in principle, conform to the requirements above. The long-term integrity of materials should be documented. Once placed, there should be a means by which the barriers can be verified”. [9]

There are different potential materials that can be suitable as barriers. The Oil & Gas UK guidelines defines a list of which materials that are suitable, and divides them into material types, depending on their chemistry and physical nature, which is shown in Table 5.1 [9].

Table 5.1: List of material types for permanent barriers (from the Oil & Gas UK guidelines (2012)) [9].

| Type | Material | Examples |
|------|---------------------------------------|--|
| A | Cement/ceramics (setting) | Portland API class cement, Pozmix, slag, phosphate cements, hardening ceramics, geopolymers. |
| B | Gouts (non-setting) | Sand or clay mixtures, bentonite pellets, barite plugs, calcium carbonate and other inert particle mixtures. |
| C | Thermosetting polymers and composites | Resins, epoxy, polyester, vinylesters, including fiber reinforcements. |
| D | Thermoplastic polymers and composites | Polyethylene, polypropylene, polyamide, PTFE, Peek, PPS, PVDF and polycarbonate, including fiber reinforcements. |
| E | Elastomeric polymers and composites | Natural rubber, neoprene, nitrile, EPDM, FKM, FFKM, silicone rubber, polyurethane, PUE and swelling rubbers, including fiber reinforcements. |
| F | Formation | Clay stone, shale, salt. |
| G | Gels | Polymer gels, polysaccharides, starches, silicate-based gels, clay-based gels, diesel/clay mixtures. |
| H | Glass | |
| I | Metals | Steel, other alloys such as bismuth-based materials. |

As stated by Syed and Cutler (2010), NORSOK lists the following five properties for the ideal sealing material for well abandonment [1]:

- *“Readily available and easily mixed*
- *Be chemically inert and non-reactive with groundwater*
- *Provide good bonding across the zones being sealed when properly placed*
- *Remain fluid proper displacement and develop adequate strength within a short period of time*
- *Have low permeability when set to resist the flow of fluid through the sealing material and the interface along the formation being sealed ” [1]*

As mentioned, the most common material used for P&A is Portland cement [9]. One of the reasons for this is that it has very similar properties to the cap rock that it is replacing. Even though cement is most

often suitable, there are some limitations and situations where cement is not the most appropriate material. Therefore alternative materials are being studied which are considered to be able to replace cement. In the next sections Portland cement and a fairly new technology, geopolymers, will be described, respectively.

5.2. Portland cement

Portland cement is an example of hydraulic cement, meaning it sets and develops comprehensive strength in contact with water [11]. One of the main advantages with this cement is that when the cement is set it is nearly insoluble in water, so when coming in contact with water the hardened material will not be destroyed. This is an essential material property when setting a plug that is needed to last “eternally”.

5.2.1. Manufacturing Portland cement

The manufacturing of Portland cement can be divided into four stages; quarrying, raw material preparation, clinkering and cement milling and storage [12]. These steps will be presented in the next sections.

Step 1: Quarrying

The first step is to quarry the raw materials used for cement into the cement factories [13]. These raw materials are limestone, clay and sand, which contain the minerals calcium, silicon, aluminum and iron. The quarried raw materials are then crushed in two stages until the materials have the size of gravel.

Step 2: Raw material preparation

This step includes pulverizing the raw materials before the calcination process of the materials in the kiln can start [11]. The calcination can be done in either a dry or a wet process. In the dry process dry materials are grinded and blended, while in the wet process these processes are done with wet slurries. It is essential to keep the materials at a homogeneous state because the kiln feed should have a very stable chemical composition.

A schematic of the dry process is shown in Fig. 5.1. In the dry process the clay and limestone are first separately crushed and dried before a test is taken to make sure that the correct amount of aluminum, iron, etc. is present, if not, materials are added [11]. Afterwards a roller mill that combines crushing, grinding, drying and size classification in one unit grinds the minerals. The raw materials are then stored in silos and are ready for the preheater. Since there might be a slight variation in the compositions of each silo, it may be required to re-blend and fine-tune the mixture before entering the kiln.

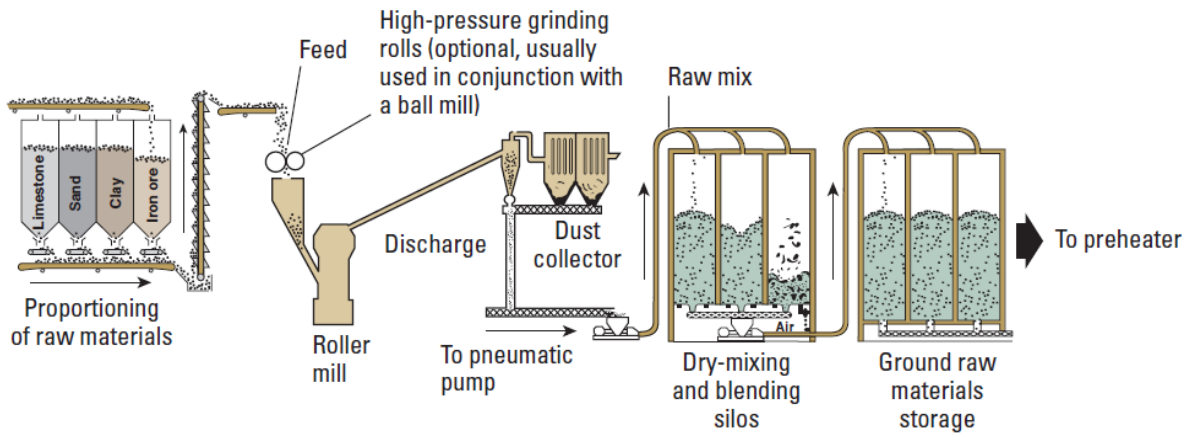


Figure 5.1: Schematic flow diagram of the dry calcination process (from Nelson and Guillot (2006)) [11].

During the wet process the dry materials are mixed with water before entering a grinding mill [11]. A schematic of the wet process is shown in Fig. 5.2. A vibration screen separates the different sizes of the grinded material, only allowing a certain size to pass through. The coarser materials are sent back to the grinding mill. To keep the mixture homogeneous, the slurry is stored in a basin with rotating arms and compressed air agitation. The slurry is tested, as for the dry state, and materials are added if necessary. It is important to be aware that the compositions may vary slightly from basin to basin. However, the final adjustments are done by blending the slurries from the different basins, before it is stored and ready for the kiln.

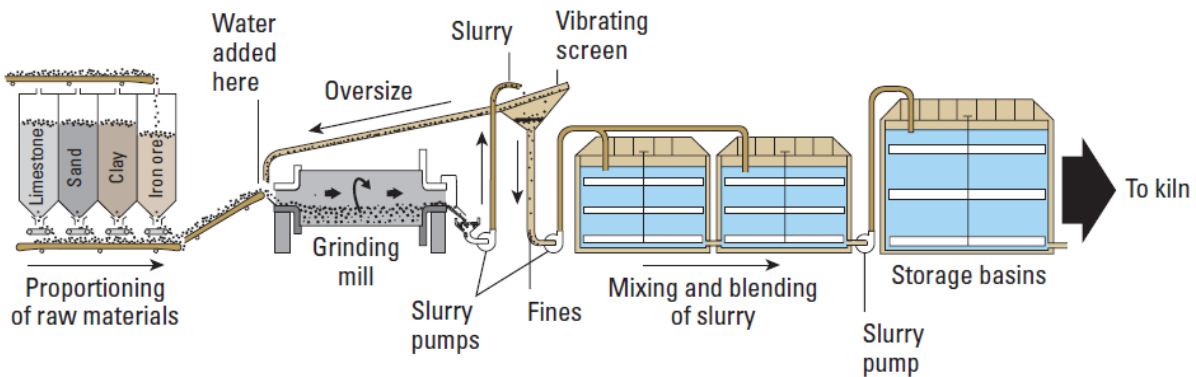


Figure 5.2: Schematic flow diagram of the wet calcination process (from Nelson and Guillot (2006)) [11].

Step 3: Clinkering

In this step the finely ground materials are dried using heaters, before they are being cooled down again [12]. The drying process involves heating the materials in a kiln to enable the sintering reactions. To ensure that the solid materials pass through the kiln, the kiln is slightly inclined [11]. A schematic flow diagram of the burning process is shown in Fig. 5.3.

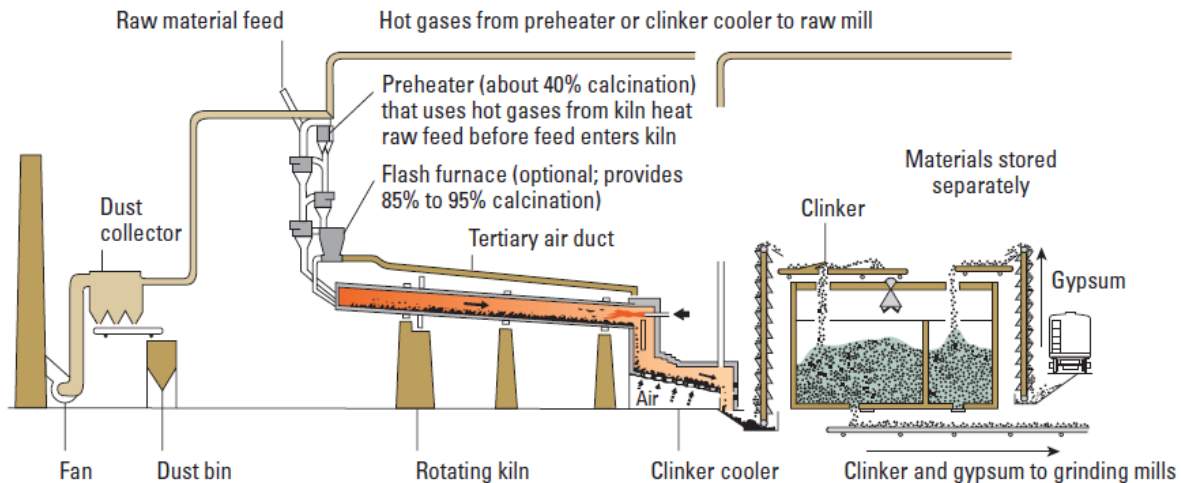


Figure 5.3: Schematic flow diagram of the burning process (from Nelson and Guillot (2006)) [11].

Sintering involves heating the materials, but not melting them, until they are fused into a solid but porous mass [11]. Before the raw materials reach the sintering stage, they go through an evaporation phase, a preheating phase, a decarbonation phase and an exothermic reaction phase. All five phases, including sintering, are essential to produce the right type of clinker for the Portland cement. During these five phases the raw materials go from a free-flowing powder where the particles are solid and do not react with each other, to a phase where the particles react and capillary forces of the liquid keep particles together and nodules are formed making a dusty clinker. To make Portland cement clinker, there is a sixth phase; the cooling phase. Here air is forced through a bed of clinker using perforated plates in the base of the cooler. The quality of the clinker is dependent on the rate of the cooling process. The best clinker is produced when the materials are cooled slowly down to 1250°C and then cooled rapidly, usually by 18-20°C/min. Slow cooling of the materials results in cement that is less hydraulically active when it is hydrated. The slow cooling results in a high compressive strength, however, the long-term strength will be low. For a rapid cooling, the early compressive strength will be lower, but the long-term strength higher.

Step 4: Cement milling and storage

The final product is produced by mixing clinker with calcium sulfate, usually gypsum [11]. The clinker, including gypsum, is then ground in large tube mills. The particle size after the grinding process varies from 1 to 100 μm . The final product is now ready for storage, and it is important that the cement is stored dry, since it reacts when coming in contact with water.

5.2.2. Portland cement materials

In cement plants clinker is produced from the heated material that exists in a rotary kiln, which again is pulverized and used in Portland cement [11]. Clinker consists of hydraulic calcium silicates, calcium aluminates and calcium aluminoferrites. The clinker contains a certain amount of calcium, silica, alumina and iron in a partly amorphous, partly crystalline condition, and these are used to be able to manufacture Portland cement. As mentioned, the finished product is produced when mixing these compounds with gypsum.

To be able to prepare a mixture that will produce clinker there have to be both calcareous materials and argillaceous materials present. Both calcareous and argillaceous materials can be found naturally or be artificially manufactured [11]. Calcareous materials contain lime, while argillaceous materials contain alumina, silica and iron oxide. Iron gives the cement a grey color and reduces the reaction temperature of the cement, while lime and silica provide the main strength of the cement [12]. The most important naturally occurring calcareous materials include sedimentary and metamorphic limestones, coral, shell deposits and “cement rock” [11]. These raw materials have a natural composition that is similar to Portland cement. The artificial raw materials are precipitated calcium carbonate and other waste products from industrial processes.

The most important naturally occurring argillaceous materials are clays, shales, marls, mudstones, slate, schist, volcanic ashes and alluvial slit [11]. The artificial sources include blast-furnace slag (BFS) and fly ash. BFS is a bi-product from steelworks, while fly ash is a bi-product from coal-fired power plants.

Due to variations in the availability of raw materials in different countries, there is a great variety of natural and artificial raw materials that are added to the oven to produce clinker for Portland cement [11]. A list of various raw materials that can be used when producing Portland cement is shown in Table 5.2 [11].

Table 5.2: Various raw materials used in producing clinker for Portland cement (from Nelson and Guillot (2006)) [11].

| Calcium | Iron | Silica | Alumina | Sulfate |
|------------------|-------------------------|------------------|----------------------|-----------------|
| Alkali waste | Blast-furnace flue dust | Calcium silicate | Aluminum-ore refuse* | Anhydrite |
| Calcite* | Clay* | Cement rock | Bauxite | Calcium sulfate |
| Cement-kiln dust | Iron ore* | Clay* | Cement rock | Gypsum* |
| Cement rock | Mill scale* | Fly ash | Clay* | |
| Chalk | Ore washings | Fuller's earth | Copper slag | |
| Clay | Pyrite cinders | Loess | Fly ash* | |
| Fuller's earth | Shale | Marl* | Fuller's earth | |
| Limestone* | | Ore washings | Loess | |
| Marble | | Quartzite | Ore washings | |
| Marl* | | Rice-hull ash | Shale* | |
| Seashells | | Sand* | Slag | |
| Shale* | | Sandstone | | |
| Slag | | Shale* | | |
| | | Slag | | |
| | | Traprock | | |

* Most common sources

To determine the properties of Portland cement the mineralogical composition of the clinker is measured. Conventionally Portland cement has the following four mineralogical compositions; alite, belite, aluminate and ferrite phase. In Table 5.3 an overview of the composition, cement notations and concentration of each mineral is listed [11]. Before deciding which raw materials and kiln fuels that should be used for the cement, it is important to be aware of what the cement is to be used for.

Table 5.3: Composition, cement notation and concentration of minerals in Portland cement
(from Nelson and Guillot (2006)) [11].

| Oxide composition | Cement notation | Common name | Concentration (wt. %) |
|---|-----------------------|---------------|-----------------------|
| $3\text{CaO} * \text{SiO}_2$ | C_3S | Alite | 55-65 |
| $2\text{CaO} * \text{SiO}_2$ | C_2S | Belite | 15-25 |
| $3\text{CaO} * \text{Al}_2\text{O}_3$ | C_3A | Aluminate | 8-14 |
| $4\text{CaO} * \text{Al}_2\text{O}_3 * \text{Fe}_2\text{O}_3$ | C_4AF | Ferrite phase | 8-12 |

5.2.3. Cement additives

Portland cement that is supposed to be used in wells must be designed to withstand a wide range of various temperatures and pressures [11]. The temperatures may vary from below freezing to 350°C and the pressure from surface pressure to more than 29 000 psi. Each well is different in both length and properties, meaning that the cement must be able to set at the right place at the right time and keep its integrity during the time for abandonment (temporary or permanently) for the different wells. To make sure that the cement fulfills all of the requirements, additives are often added to the cement mixture. The additives may change the abilities of the cement and help to get a successful placement of the cement plug under the different conditions. There are over a hundred such additives available today, and they can mainly be divided into eight categories; accelerators, retarders, extenders, weighting agents, dispersants, fluid loss control agents, lost circulation control agents and specialty additives. These eight categories will be discussed briefly in the next section.

5.2.3.1. Accelerators

Accelerators are chemicals that can increase the strength development and reduce the setting time of the cement [11]. They may be used to counter out the delay in cement setting caused by other additives. The most common inorganic salt to be used as accelerator is sodium chloride (NaCl). The different salts work as accelerators at different concentrations, meaning that for a certain concentration, it may change its properties to be unfavorable. An example is when a concentration of 15% NaCl is used it acts as an accelerator, but if the concentration exceeds 20% it will change its properties and act as a retarder. In this thesis water glass and sodium hydroxide (NaOH) are used as accelerators.

5.2.3.2. Retarders

Retarders are used to delay the setting time of the cement [11]. The process of explaining the effect that the retarders have on the curing process is still not defined. There have been proposed several different theories, but still, none of them can fully explain the process. In Nelson and Guillot (2004) four of the proposed theories have been shortly described [11]:

- a) *“Adsorption theory: The retarder adsorbs onto the surfaces of the hydration products, thereby inhibiting contact with water.*
- b) *Precipitation theory: The retarder reacts with calcium ions, hydroxyl ions, or both in the aqueous phase, forming an insoluble and impermeable layer around the cement grains.*
- c) *Nucleation theory: The retarder adsorbs onto the nuclei of hydration products, arresting their future growth.*
- d) *Complexation theory: The retarder chelates the calcium ions, preventing the formation of nuclei”* [11].

Even though the theories are different, there may be seen a small similarity in them; dissolving and absorption of salts that prevents the hydration process [11]. The most commonly used retarders for well cements are the sodium and calcium salts of lignosulfonic acids.

5.2.3.3. Extenders

Extenders can have several functions such as lowering the density of a cement system, reducing the quantity of cement per unit volume of set product, or both [11]. The reduced slurry density will reduce the hydrostatic pressure during cementing and thereby prevent lost circulation due to weak formations. The extenders are divided into three groups; water extenders, low-density aggregates and gaseous extenders. Water extenders are clays and other water viscosifying agents that allow more water to bind to the cement system. This helps to maintain homogeneous slurry and prevent the production of free water. The low-density groups are aggregates with a density lower than Portland cement ($3,2 \text{ g/cm}^3$), and are used in large amounts to reduce the slurry density. Gaseous extenders are foamed cements prepared using nitrogen or air that gives the cement a low density yet a good compressive strength.

Probably the most important group of extenders is pozzolans. Pozzolans may also be known as alkali-activated binders. According to Nelson and Guillot (2006) pozzolans are defined as [11]:

“A siliceous or siliceous and aluminous material that possesses little or no cementitious value, but will in a finely divided form and in the presence of moisture, chemically react with calcium hydroxide to form compounds possessing cementitious properties” [11].

During cement hydration calcium hydroxide will be released and removed by the water that is in contact with the cement [11]. This leads to a reduction in the compressive strength. However, when pozzolans are present, they prevent the calcium hydroxide from escaping; hence, there is a build-up in the compressive strength. The cement system then becomes a stable and very durable compound with a low permeability. There are two main classes of pozzolans; natural and artificial pozzolans. Natural pozzolans are volcanic ashes and diatomaceous earth and artificial pozzolans include for example metakaolin and fly ash. Both fly ash and metakaolin are used in the experiments in this thesis.

In the last years the interest in investigating the effect of alkali-activated binders has increased. Experimental investigations on determining the reactivity of different raw materials have, among others, been performed by Buchwald et al. [14]. In their test the released concentration of silicate and aluminate monomers by alkaline solutions were determined. They used five different raw materials; metakaolin, slag, fly ash, brick powder and thermal activated clay. Their results showed that metakaolin released the highest amount per weight of silicate and aluminate, followed by fly ash. However, fly ash needed more time before the monomers were detectable in the solution due to the smaller surface area and higher stability of the glassy phase in fly ash compared to metakaolin. The amount of released silicate and aluminate in the thermal activated clay and the brick powder was almost the same. This can be explained by the almost identical chemical and phase compositions of the two materials. For the slag, the amount released was quite low, and did not change over the contact time. It was also found that the strength increased, for all five materials, when the content of sodium hydroxide increased. This showed that the building of calcium silica hydrate phases and calcium aluminate hydrate phases leads to good strength performance.

5.2.3.4. Weighting agents

In some wells there is a need to increase the slurry density to avoid a decrease in the hydrostatic pressure that may cause an uncontrolled situation of a well [11]. One way to reduce the slurry density is to reduce the amount of mix water. Another alternative is adding weighting agents. These weighting agents have to have a particle size distribution that is compatible with the cement, have a low mix water requirement, be compatible with other cement additives that may be present and be inert, due to cement hydration. The most common weighting agents are ilmenite, barite and manganese tetraoxide.

5.2.3.5. Dispersants

Some cement slurries are highly viscous due to the high concentration of suspended particles and solid volume fraction [11]. Highly viscous slurries may cause problems during placement of the cement, especially in long and inclined wells. To reduce the viscosity of the cement slurry, dispersants can be added. The most commonly used dispersant is polynaphthalene sulfonate. It is very cost effective; however, because of its toxicity to algae, it is less used in marine environments. Other commonly used dispersants are lignosulfonates and hydroxycarboxylic acids. But there is a problem related to these as well; they have shown to have a retarding effect, meaning that they reduce the setting time of the cement.

5.2.3.6. Fluid loss control agents

Both during and after cement placement, some of the aqueous phase from the slurry will escape to the formation and this is called fluid loss [11]. It is important to avoid high fluid losses to prevent well problems. One problem may be that there is such high fluid loss when pumping down the cement that the density of the slurry increases significantly, leading to difficulty with pumping it further down to the right position. The fluid loss may also change the design properties of the slurry which can lead to poor sealing of the well. To prevent these problems fluid loss control agents may be added to the cement slurry. The exact mechanism that occurs are not yet completely understood, however there are some processes that are known to occur. The particles in the fluid loss control agents can reduce the filter cake permeability or increase the viscosity of the aqueous phase, or both.

The most commonly used fluid loss control agents are divided into two classes; finely divided particulate materials and water-soluble polymers [11]. The water-soluble polymers that are used may be both natural and synthetic. The most widely used particulate materials are bentonite, carbonate, carbon black, micro silica, asphaltene, and thermoplastic resins. Micro silica is used in this thesis.

5.2.3.7. *Lost circulation control agents*

Lost circulation is a serious problem during cementing [11]. When performing a primary cementing job there is often a need for remedial cementing due to the lost circulation. Lost circulations often occur in weak, highly permeable and fractured zones. To prevent this, materials that bridge over fractures and blocks weak zones are added. The materials increase the resistance of the zone against pressure. Commonly used bridging agents are granular materials, such as gilsonite and granular coal. If the cavernous zones are so large that the bridging agents cannot prevent lost circulation, thixotropic cements are used. When thixotropic is used in the slurry it will no longer be subjected to shear and the slurry will therefore take a gel form and become self-supporting. The thixotropic cement will eventually plug the lost circulation.

5.2.3.8. *Specialty additives*

There are still a number of materials that do not fit into the already mentioned categories [11]. These materials are called specialty additives. These include antifoam agents, fibrous materials that are used to increase the resistance to the stresses associated with perforating, hydraulic fracturing, and formation movement, radioactive tracing agents that are used to easier locate the plug and mud decontaminants that are used to reduce retardation of the cement slurry when mixed with drilling fluid.

5.3. Geopolymers

“Geopolymer technology” is the term for cement made up of aluminum and silicon, instead of calcium and silicon [15]. Geopolymers are a type of inorganic polymers that can be formed at room temperature using industrial waste or by-products as source material. In the recent years there has been a higher awareness on the hazardous solid waste generation and its impact on human health, as well as an increased focus on the environmental consequences of waste disposal [16]. This forces the industry to find alternative ways to reuse waste materials. One solution is to reuse the waste materials and the by-products containing heavy metals to create geopolymers as an alternative to Portland cement. Geopolymers can be used in building roads, construction and offshore operations.

5.3.1. *Raw materials for geopolymers*

There are several different minerals that can be used as raw materials in geopolymers [17]. The most important factor is that the materials contain silica and alumina [16]. The minerals may be of natural origins, like kaolinite or calcined kaolinite (metakaolin) or industrial by-products, like BFS, from the iron-steel making industry, and fly ash, from the combustion of coal. Fly ash and BFS are the most readily available raw materials [15].

5.3.2. Manufacturing geopolymers

Geopolymers are formed from geopolymerization, which is a reaction that chemically integrates minerals involving naturally occurring silica-aluminates [16]. Geopolymerization can mainly be divided into three stages; dissolution, condensation and polymerization. During the first stage, dissolution, the source of silica and alumina reacts and dissolves silicon and aluminum ions in an alkaline solution [18]. In the next stage, condensation, the solution that is formed reacts and forms oxygen bonds between the silicon and aluminum molecules lying next to each other. During the last stage, polymerization, heat is applied to the solution (usually up to 90°C) and the molecules form rigid chains of oxygen bonding. The reaction forms molecules with a structure similar to those building natural rocks [15]. These inorganic polymeric materials can be considered as an amorphous equivalent of geological feldspars, and these are called “geopolymers”.

According to Khale and Chaudary (2007) the geopolymerization can be affected by several parameters [16]:

- Temperature: Several researchers have shown that higher curing temperature increases the compressive strength. The high temperature may also reduce the curing time. Experiments conducted by Brooks showed that the curing time of fly ash was reduced by a factor of six when the temperature was increased from 6°C to 80°C.
- Curing time: Longer curing time improves the polymerization process, increasing the compressive strength. However, if the geopolymer is exposed to high temperature for a long period of time, the granular structure in the geopolymers can break, resulting in dehydration and shrinkage.
- Alkali solution concentration: This is the most important factor during geopolymerization. A higher concentration of hydroxide ion concentration increases the solubility of aluminum-silicates, resulting in increased compressive strength. However, the compressive strength has shown to decrease if the concentration becomes too high, due to excess alkali ions in the framework.
- pH: Increased pH of the activating solution decreases the setting time of the cement. Observations have shown that a pH at 13-14 increases the compressive strength the most for geopolymers.

- Silicate and aluminum ratio: To create good bonding and high strength it is important to have aluminum-silicate present. A high content of highly soluble silicate will provide the solution with aluminum-silicates. According to Khale and Chaudhary (2007) an aluminum-silicate ratio of 3,16-3,46 will optimize the compressive strength.
- Solid-liquid ratio: As for cement, the compressive strength of geopolymers decreases with an increased amount of water.

5.3.3. Geopolymers properties

Geopolymers have shown to give a comparable performance compared to the traditional cement binders in Portland cement [15]. One of the main differences between Portland cement and geopolymers is related to the greenhouse emissions. Portland cement is dependent on high-energy manufacturing processes, meaning that it requires large amounts of energy to produce it [15]. Geopolymers, on the other hand, uses low energy materials, so it is possible to save a large amount of energy when producing geopolymers. It has shown that the CO₂ emission is reduced with about 80% compared to that of ordinary Portland cement [16]. In addition, geopolymers uses by-products from other manufactures, such as fly ash and BFS [19]. Geopolymers have also shown to give high compressive strength, low shrinkage, be acid resistant, fire resistant, have low thermal conductivity and be environmental friendly. However, it should be noted that the technical benefits of geopolymers may vary depending on the raw materials and the processing conditions.

The compressive strength in geopolymers has shown to be dependent on the curing temperature. Experimental work presented by Rovnanik (2009) on geopolymer based metakaolin showed that the curing temperature has an essential effect on setting and hardening [20]. Higher temperatures increase the early age development of compressive and flexural strengths. However, early hardening led to larger pores and an increase in cumulative pore volume which showed to have a negative effect on the final mechanical properties of the geopolymer material. In other words, the interaction of various parameters on the workability and compressive strength of geopolymers is complex and there is a need for computing several studies on the subject.

6. Experimental conditions

6.1. Materials

The materials used during the experiments were fly ash, BFS, metakaolin, water glass, silicon dioxide and NaOH. The materials will be described briefly in the next sections.

6.1.1. Fly ash

Fly ash is a synthetically made pozzolan. It is the byproduct from burning pulverized coal in power plants [11]. The mineral impurities in the coal (clay, feldspar, quartz and shale) fuse and fly out during the burning process. The “flying” ash from the power plant is captured and the minerals are cooled and solidified into spherical glassy particles, and this is called fly ash [21]. The main compositions of fly ashes are silica and alumina with some iron oxide, lime, alkalis, and magnesia [11]. There are also found quartz, mullite, hematite, and magnetite, as well as some combustible matter. Depending on the source of the coal that is used in the power plant, the fly ash composition and property may vary. The fine powder of fly ash resembles Portland cement, but from a chemically point of view it is different [21]. When fly ash comes in contact with calcium hydroxide, a chemical reaction occurs. The reaction prevents calcium hydroxide from escaping from the geopolymers and thereby improves the performance of concrete, making it stronger, more durable, and more resistant to chemical attacks. Fly ash also has a great benefit regarding the environment. However, the reaction is slow, resulting in a delay in hardening of the geopolymers which may be a challenge when setting a well plug. In many cases, the final hardened structure is formed before the dissolution of fly ash is completed.

According to American Society for Testing and Minerals International (ASTM), there are three categories of fly ash and these are class N, F and C [11]. The most used type in well cementing is type F. The different classes are separated due to their chemical grounds. In Table 6.1 an overview of the three classes and their chemical requirements are shown. Class C ashes are produced from lignite or subbituminous coals and class N and F ashes from burning anthracite or bituminous coals.

Table 6.1: Chemical requirements for fly ashes (from Nelson and Guillot (2006)) [11].

| | Class N | Class F | Class C |
|---|---------|---------|---------|
| Minimum silicon dioxide + aluminum oxide+ iron oxide (%) | 70 | 70 | 50 |
| Maximum sulfur trioxide (%) | 4 | 5 | 5 |
| Maximum moisture content (%) | 3 | 3 | 3 |
| Maximum loss on ignition (%) | 10 | 12 | 6 |

During the experiments fly ash class C and F were used. Class C was delivered by NORCEM, Sweden, while the supplier of class F is unspecified.

6.1.2. Blast Furnace Slag

BFS is a byproduct from iron making in a blast furnace [11]. BFS can be used as a replacement for, or be blended with, Portland cement. When blended with Portland cement it is called Portland slag cements. Using BFS has shown improvements in some properties in the cement, like being more resistant to chemical attacks and having both environmental and economic benefits.

During the production of iron, the blast furnace is fueled with iron ore, coke and flux (limestone and/or dolomite) [22]. During the melting process in the furnace a chemical combination of calcium and magnesium oxides from the flux and alumina and silica is formed from the ore and coke ash, and this is what is called BFS. The compositions of BFS may vary due to different iron ore sources.

The type of BFS may be varied due to the cooling process [22]. Slow cooling will crystallize the slag into a material having virtually no cementitious properties, while rapid cooling will form a glass that is latent hydraulic cement [11]. Latent hydraulic cement means that it needs more than only water to set, it requires a chemical activation. The different chemical activators that can be used are sodium hydroxide, sodium carbonate, sodium silicate, sodium sulfate, calcium sulfate, lime, or mixtures thereof. Portland cement is also an effective activator, due to gypsum (sulfate activation) and portlandite. Therefore, when blending BFS with Portland cement, there is generally no need for adding activators. The amount of BFS added to Portland cement may vary from 80% to less than 50%, which is most common. Portland slag cement has a reduced porosity due to smaller pore sizes.

As mentioned, one benefit of using BFS blended with Portland cement is that the Portland slag cement is more resistant to chemical attacks. Other benefits pointed out by Neslon and Gulliot (2008) are [11]:

- *“Better sulfate resistance*
- *Slower diffusion of chloride and alkali ions through the cement matrix*
- *Lower set-cement permeability “[11].*

The BFS that was used in the four first tests (no.58, 62, 76 and 87) during the experiments is unidentified, while for the rest of the tests there was used BFS delivered by Merox in Oxelösund, Sweden.

6.1.3. Metakaolin

Metakaolin is a dehydroxylated form of clay mineral kaolinite [23]. The calcination of kaolinite forms an amorphous material called metakaolin. This is done at temperatures between 600-850°C. Metakaolin is a reactive pozzolanic material. Metakaolin can be used in cement where it will react with the cement and the lime present. The main advantages when using metakaolin are [24]:

- Improved the strength due to the rapid build-up of compressive strength
- Improved durability: the pozzolanic and hydraulic reactions of metakaolin leads to greater impermeability
- Contributions to sustainability: the low process temperature of metakaolin saves large amounts of energy and reduces the greenhouse gas emissions.

During the experiments in this thesis kaolin delivered by Merck (Germany) was used. Through calcination of kaolin, metakaolin (MK-750) was made. Kaolin was heated up to 750°C for 6 hours and then cooled for 6 hours. The name MK-750 describes that kaolin was calcined using 750°C.

6.1.4. Water glass

Water glass, also known as sodium silicate, contains compounds of sodium oxide (Na_2O) and silica (SiO_2) that forms a glassy solid material that is soluble in water [25]. Water glass can be produced as both an aqueous solution and as solid material. Water glass is produced when burning sodium carbonate and silica sand in a furnace at temperatures between 1000-1400°C. The process gives off carbon dioxide and produces sodium silicate. Another method to form water glass is to dissolve silica under pressure in a heated aqueous solution of NaOH.

The viscosity of the solution depends on the ratio of SiO_2 and Na_2O ; the higher concentration of both, the more viscous solution [25]. When water glass comes in contact with water it dissolves and produces an

alkaline solution which is glassy and colorless. Due to the alkali properties, water glass will react under acidic conditions and form a hard glassy gel, which is a very useful bonding agent for cement. Water glass is used in several different industrial products, such as, laundry detergents, as flocculants in water-treatment plants and as a binder and adhesive, because of its convenient source of sodium.

Water glass used during the experiments was delivered by Merck KGaA (Germany).

6.1.5. Silicon dioxide

SiO₂, also known as silica, is the most abundant mineral in the Earth's crust [26]. Silica is one of the most commonly encountered substances in daily life and it is used in numerous applications, such as, to make glass, in toothpaste to scrub away plaque on teeth and as an ingredient in cement. Silica is mostly harmless; however, in powder form it may pose a risk if it is inhaled over time. When inhaled it may cause a condition called silicosis, which causes shortness of breath, fever, and coughing and causes the skin to turn blue.

Silica can be found in various forms worldwide, and it mostly forms in nature [26]. There are two types of silica that are found in nature; granular silicon dioxide and crystalline silicon dioxide. Granular silicon dioxide is commonly known as sand, while crystalline silicon dioxide is known as quartz crystal with a milky clear color. Both types have the same chemical makeup and generally the same properties. The main reason that they are slightly different is that they are formed differently. Silica is manufactured in several forms including fused quartz, crystal, fumed silica, silica gel, colloidal silica and aerogel [27]. Silica is formed by strong, directional covalent bonds between four oxygen atoms and one silicon atom [26]. Therefore, when using silica in cement it will make the concrete stronger. Because of the strong bonding silica is a very hard mineral and it is also highly resistant to heat, with a melting point of 1650°C.

In the experiments quartz was used as silica source and it was delivered by Sigma-Aldrich (Germany).

6.1.6. Micro silica

Micro silica, also known as silica fume, is a fine pozzolanic material [28]. It is a byproduct produced when silicon is manufactured in an electric furnace. During the production, silica fume rises as an oxidized vapor from the furnaces. After it has cooled it condenses and it can then be collected and stored. Before the final product, micro silica can be used, impurities are removed and the particle size is controlled. Micro silica is available in both solid and liquid form, whereas liquid form is the most common. It contains mostly SiO₂, usually 85% or more.

Micro silica can be used in several cementitious products, such as concrete, ceramic and polymers [28]. Usually about 5-10% micro silica by mass of the total cementitious material is used. When micro silica used in concrete is combined with calcium hydroxide it forms calcium hydrate through pozzolanic reactions, which results in a denser and stronger material. Micro silica also increases the impermeability of the concrete, due to its small particle size compared to the cement particles.

The micro silica used during the experiments was delivered by Elkem (Kristiansand, Norway) and had a grade of 955. The composition of the micro silica used is presented in Table 6.2.

Table 6.2: Composition of micro silica delivered by Elkem (Norway).

| Name | Formula | Percentage |
|------------------------|--------------------------------|-------------------|
| Silica | SiO ₂ | Min. 95.5% |
| Carbon | C | Max. 1% |
| Iron oxide | Fe ₂ O ₃ | Max 0.3% |
| Aluminum oxide | Al ₂ O ₃ | Max 0.7% |
| Calcium oxide | CaO | Max 0.4% |
| Magnesium oxide | MgO | Max 0.5% |
| Potassium oxide | K ₂ O | Max. 1% |
| Sodium oxide | Na ₂ O | Max. 0.4% |

6.1.7. Sodium hydroxide

NaOH, also known as caustic soda, is a white material commonly found in the form of pellets, granules or flakes [29]. NaOH is highly soluble in water and because of its high alkaline activator levels; it is often used in geopolymer mixtures. The NaOH concentration has a significant effect on the compressive strength of geopolymers. As mentioned earlier, Buchwald et al. found that the compressive strength increased for five different materials (metakaolin, fly ash, slag, thermal activated clay and brick powder) by an increasing NaOH concentration [14]. However, only metakaolin could produce compressive strength with NaOH/solid concentrations higher than 20%, which indicates that the concentration ratio is an important factor to achieve the positive effect of NaOH.

During these experiments a 6M, 8M and 10M NaOH solution were used. The NaOH was delivered by Merck KGaA (Germany).

6.2. Equipment

An Ultrasonic Cement Analyzer (UCA) was used to measure the compressive strength of the geopolymer plugs and a Toni Technic was used to perform Uniaxial Compressive Strength (UCS) tests of the plugs. The UCA and the UCS test will be shortly described in the next section.

6.2.1. Ultrasonic Cement Analyzer

UCA is a non-destructive test method that measures the change in velocity of an ultrasonic signal under simulated temperature and pressure conditions.

Fig. 6.1 illustrates a UCA showing the current temperature and pressure conditions for the system. It is important to take notice that the temperature is independent of the rest of the system. Fig. 6.2 shows the pressure controller of the UCA system. The pressure controller makes it possible to regulate the pressure conditions of the system at all times. However, it is important to take notice that since there may be several UCA systems connected to the same pressure controller, a pressure decrease in one system will affect the pressure in the two other systems. In our experiments, three UCA systems were connected.



Figure 6.1: Ultrasonic Cement Analyzer (UCA) system.

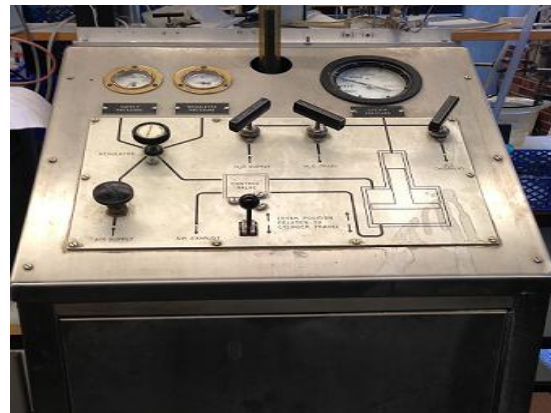


Figure 6.2: Pressure controller connected to the UCA system.

After mixing the cement slurry it is immediately placed in a sample holder to avoid that the cement sets. Afterwards the holder is placed in the UCA system and ultrasonic waves are continuously sent through the sample [30]. The ultrasonic waves collect information regarding curing time, maximum compressive strength and the early strength buildup. The system uses an empirical relationship between the compressive strength and the transit time data for different cement slurry systems and the sonic strength is correlated to transit time [11]. The strength of the slurry will increase during time, making the signal to travel faster through the sample [30]. All collected data are sent to a computer that shows the

data in real time. The data is illustrated in a graph with the compressive strength, temperature and transit time as function of time.

The main advantages with this method are [30]:

- Non-destructive: the cement samples are not destroyed during testing
- Flexible: by adding additional autoclaves, the system can perform up to four tests at the same time
- Realistic: the temperature and pressure are set to simulate downhole conditions
- Accurate data: the unique technology gives a clean signal leading to more accurate times and data
- Computer controlled: data is instantly available and shown at the computer for easy analysis

Disadvantages with this system is that it does not take into account the tri-axial loading that the cement will experience in the wellbore, meaning the failure stresses may be different from those observed in the UCA test [11]. The UCA system also do not account for the shear strength of the casing to cement or the casing to formation bond.

The UCAs used during these experiments were borrowed from Halliburton Services.

6.2.2. Uniaxial Compressive Strength

The UCS test is a destructive, unsupported test [31]. The sample is loaded axially until failure or the sample is deformed. To be able to obtain an even load distribution and get accurate results, it is essential that the top and bottom of the sample is flat and smooth [31]. This was ensured by cutting the samples with a diamond blade cutter during the experiments. It is also important that the sample is positioned in the center of the UCS tester to evenly distribute the applied force throughout the sample [31]. The applied force is registered on a computer and illustrated in a graphical presentation. This method gives good mechanical strength measurements.

The instrument used to measure the UCS in these experiments was a Toni Technic. The Toni Technic has a strength limit at 3000 kN.

6.3. Mixing procedure

The same mixing procedure was used when preparing samples for both the UCA and UCS tests.

The materials were all weighed using a Mettler Toledo weight and mixed using a Hamilton Beach Scovill mixer. The following steps were made when preparing the geopolymer mixture:

- 1) Weighed the materials, both solids and liquids
- 2) Mixed the liquid materials in a container
- 3) Added the solid materials while mixing the geopolymers with a spoon. Added the solids in the following order:
 - a. Fly ash
 - b. BFS
 - c. MK-750
 - d. Silica (SiO_2)
- 4) Mixed the slurry at speed “Medium” (M) on the Hamilton Beach Scovill mixer
- 5) Ensured that there was no residual solids stuck on the wall or in the bottom of the container, and if there was, the mixer was stopped and the materials were stirred into the mixture with a spoon
- 6) Increased the speed up to “High” (H) on the mixer and left the slurry in the mixer until the slurry was uniformly mixed
- 7) Poured the mixture in the already prepared relevant containers (for either UCA or UCS tests)

Due to the fact that some of the geopolymers had short setting time, it was important to put the slurry into the relevant container as soon as possible after being mixed.

6.4. Test results

6.4.1. Ultrasonic Cement Analyzer test

To find a suitable recipe with high compressive strength measurements, several experiments were carried out. The UCA measured the compressive strength development throughout the curing of the geopolymer plug. If the desired strength was not reached, adjustments were made to the recipe to try to increase the compressive strength. All tests were carried out at a curing temperature of 88°C and at a pressure of approximately 5100 psi. The method of correlation that was used in the UCA was cement slurry type C. The original graphs from the UCA tests can be found in Appendix A.

The solid-liquid ratio was also calculated for each test using the following equation:

$$SLR = \frac{\sum \text{mass of solid [g]}}{\sum \text{mass of liquid [g]}} \quad (1)$$

6.4.1.1. Recipes

The recipes and the calculated SLR of the different samples are presented in Table 6.3. It should be noted that in the sample no. 100 and no. 130 fly ash F was replaced by fly ash C and silica was replaced by micro silica. During the experiment it was desired that the SLR was kept constant. However, a lower SLR was tested in no. 84 and 87 to see the effect of this parameter. The low SLR resulted in lower compressive strength, which is illustrated in the next sections. The SLR was thereby increased to the same value as the previous tests in test no. 100 and then increased even more in test no. 130. This was done to see how an even higher SLR would affect the strength.

Table 6.3: Recipes and solid-liquid ratio of the samples.

| Test no. | No. 58 | No. 62 | No. 76 | No. 84 | No. 87 | No. 100 | No. 130 |
|--------------------------------|--------|--------|--------|--------|--------|---------|---------|
| 8M NaOH (g) | 112.5 | 112.6 | 121.6 | 150.8 | 150.5 | 153.2 | 87.8 |
| Water glass (g) | 112.5 | 112.5 | 121.7 | 150.3 | 150.3 | 91.9 | 87.8 |
| Fly ash F (g) | 130.0 | 175.0 | 130.3 | 130.0 | 130.1 | 130.0* | 369.0* |
| BFS (g) | 76.6 | 76.6 | 76.6 | 76.1 | 76.1 | 76.6 | 0.0 |
| MK-750 (g) | 45.0 | 0.0 | 62.9 | 80.2 | 80.2 | 63.0 | 0.0 |
| Silica (SiO ₂) (g) | 45.3 | 45.3 | 45.3 | 36.0 | 36.0 | 45.3* | 0.0 |
| SLR | 1.3 | 1.3 | 1.3 | 1.1 | 1.1 | 1.3 | 2.1 |

*Two new parameters; fly ash C and micro silica

6.4.1.2. Results

Test number 58

In Fig. 6.3 the compressive strength in psi is plotted against time. The key features from the original graph from the UCA test are tabulated in Appendix A, is shown in Table 6.4.

The test lasted approximately 144 hours. It is found from the Fig. 6.3 that the onset of the strength buildup was approximately after 2 hours. The strength builds rapidly up until it reaches a highest point of 1958 psi after approximately 42 hours. Afterwards the strength starts to decrease slightly and when the test endend, after approximately 144 hours, the compressice stregth was 1567 psi and still decreasing.

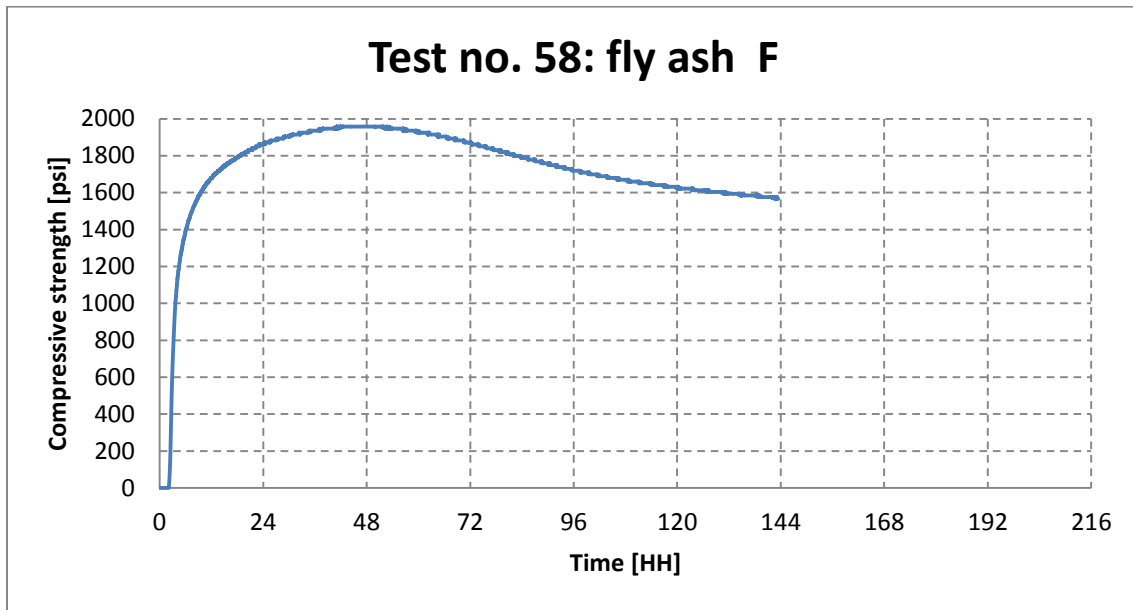


Figure 6.3: Graphical presentation of the result from the UCA test of sample no. 58. Performed at a curing pressure of 5100 psi and curing temperature of 88°C.

Table 6.4: Key features from the original graph are tabulated in Appendix A, for test no. 58.

| | Strength (psi) | Transit time (ms/in) | Temperature (°C) | Time (HH:MM) |
|------------------------------------|-------------------|-------------------------|---------------------|-----------------|
| 50 psi | 50 | 11.5 | 85 | 2:15 |
| 500 psi | 500 | 10.5 | 89 | 2:47 |
| Max strength | 1958 | 9.0 | 88 | 41:29 |
| Reached curing temp. (88°C) | 111 | 11.3 | 88 | 2:22 |
| End point | 1503 | 9.4 | 88 | 143:29 |

Test number 62

A graphical presentation of the compressive strength in psi as function of time is shown in Fig. 6.4. The key features from the original graph are tabulated in Appendix A, is shown in Table 6.5.

The test lasted approximately 244 hours. The onset of the strength buildup was approximately after 2 hours. The compressive strength builds rapidly up until it reaches its highest point at 1684 psi after 13 hours. The strength then decreases quickly until it reaches 958 psi after approximately 51 hours. Afterwards the strength slightly increases again and after 244 hours it was 1160 psi and still increasing.

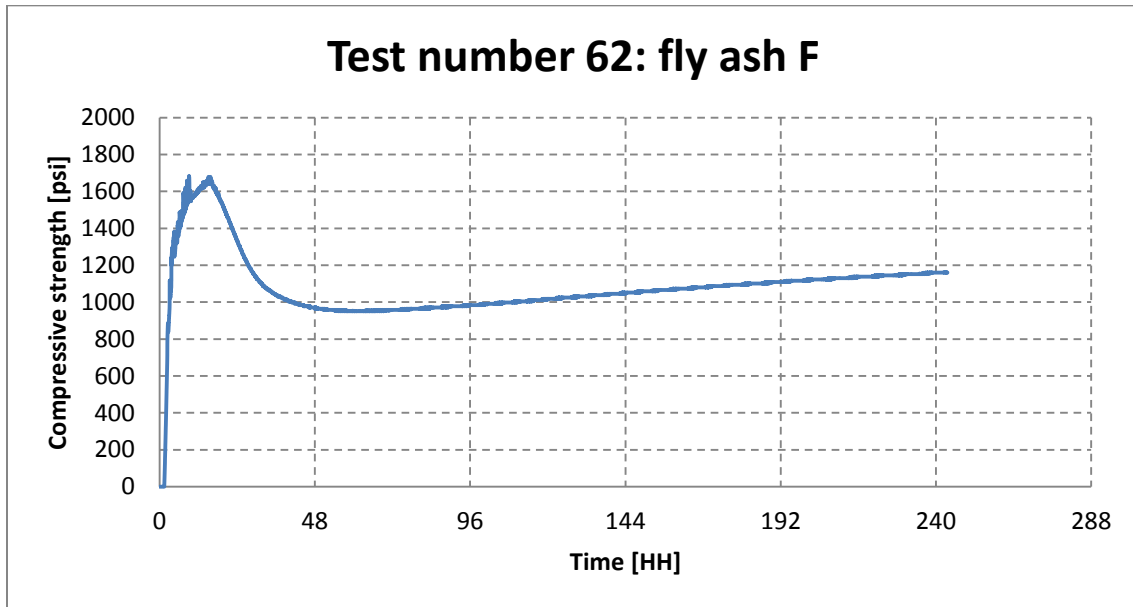


Figure 6.4: Graphical presentation of the result from the UCA test of sample no. 62. Performed at a curing pressure of 5100 psi and curing temperature of 88°C.

Table 6.5: Key features from the original graph are tabulated in Appendix A, for test no. 62.

| | Strength (psi) | Transit time (ms/in) | Temperature (°C) | Time (HH:MM) |
|------------------------------------|-------------------|-------------------------|---------------------|-----------------|
| 50 psi | 50 | 11.4 | 76 | 1:30 |
| 500 psi | 500 | 10.5 | 90 | 2:07 |
| Max strength | 1684 | 9.2 | 88 | 9:04 |
| Reached curing temp. (88°C) | 353 | 10.8 | 88 | 1:55 |
| End point | 1160 | 9.7 | 88 | 243:34 |

Test number 76

Due to a defect own in the UCA, a heating bath was used to heat up the sample instead. This resulted in a curing temperature of 85°C and the time to reach the curing temperature increased quite much. Fig. 6.5 illustrates the compressive strength in psi as function of time. It should be pointed out that the scale of the compressive strength in Fig. 6.5 is higher than for the figures from the other tests. The key features from the original graph are tabulated in Appendix A, is shown in Table 6.6.

The test lasted approximately 191 hours. The onset of the strength buildup was after approximately 3 hours. The compressive strength builds rapidly up to 1990 psi during the first 57 hours. Afterwards the strength decreases slowly and when the test ended, the strength was 1626 psi and still decreasing.

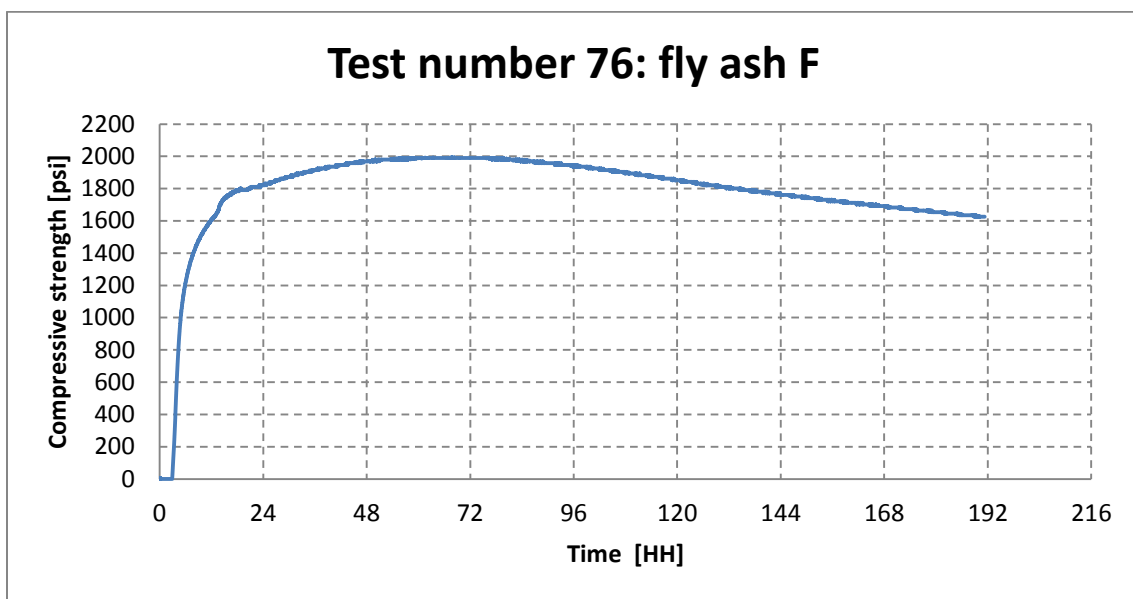


Figure 6.5: Graphical presentation of the result from the UCA test of sample no. 76. Performed at a curing pressure of 5100 psi and curing temperature of 88°C.

Table 6.6: Key features from the original graph are tabulated in Appendix A, for test no. 76.

| | Strength (psi) | Transit time (ms/in) | Temperature (°C) | Time (HH:MM) |
|------------------------------------|----------------|----------------------|------------------|--------------|
| 50 psi | 50 | 11.5 | 70 | 3:00 |
| 500 psi | 500 | 10.6 | 84 | 3:47 |
| Max strength | 1990 | 9.0 | 87 | 57:08 |
| Reached curing temp. (85°C) | 682 | 10.3 | 85 | 4:05 |
| End point | 1626 | 9.3 | 87 | 191:17 |

Test number 84

A graphical presentation of the compressive strength in psi as function of time is shown in Fig. 6.6. The key features from the original graph are tabulated in Appendix A, is shown in Table 6.7.

Due to unforeseen loss of pressure because of leakage, the test failed after approximately 50 hours. The onset of the strength buildup was after approximately 2 hours. The compressive strength builds rapidly up until it reached 1151 psi. Afterwards the compressive strength is quite unstable due to the unforeseen pressure loss. When the test stopped, after approximately 50 hours, the strength was 797 psi.

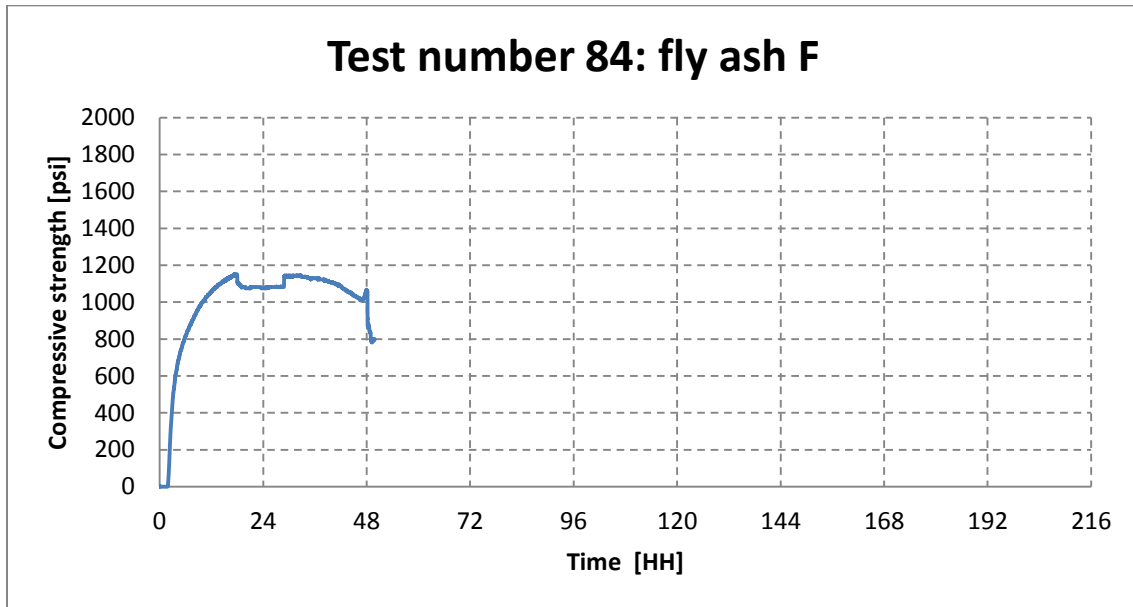


Figure 6.6: Graphical presentation of the result from the UCA test of sample no. 84. Performed at a curing pressure of 5100 psi and curing temperature of 88°C.

Table 6.7: Key features from the original graph are tabulated in Appendix A, for test no. 84.

| | Strength (psi) | Transit time (ms/in) | Temperature (°C) | Time (HH:MM) |
|------------------------------------|---------------------------|---------------------------------|-----------------------------|-------------------------|
| 50 psi | 50 | 11.7 | 88 | 2:02 |
| 500 psi | 500 | 10.7 | 88 | 3:08 |
| Max strength | 1151 | 9.8 | 88 | 17:18 |
| Reached curing temp. (88°C) | 37 | 11.7 | 88 | 2:00 |
| End point | 797 | 10.2 | 54 | 49:49 |

Test number 87

Because test no. 84 failed, an equal test, using the same recipe was performed.

A graphical presentation of the compressive strength in psi as function of time is shown in Fig. 6.7. The key features from the original graph are tabulated in Appendix A, is shown in Table 6.8.

The test lasted approximately 167 hours. The onset of the strength buildup was after approximately 2 hours. The compressive strength builds rapidly up to 1144 psi during the first 33 hours, before it starts to decrease slightly until it reaches 374 psi. After about 94 hours it starts to slightly increase again. When the test ended, after approximately 167, the strength reached 444 psi and still increasing.

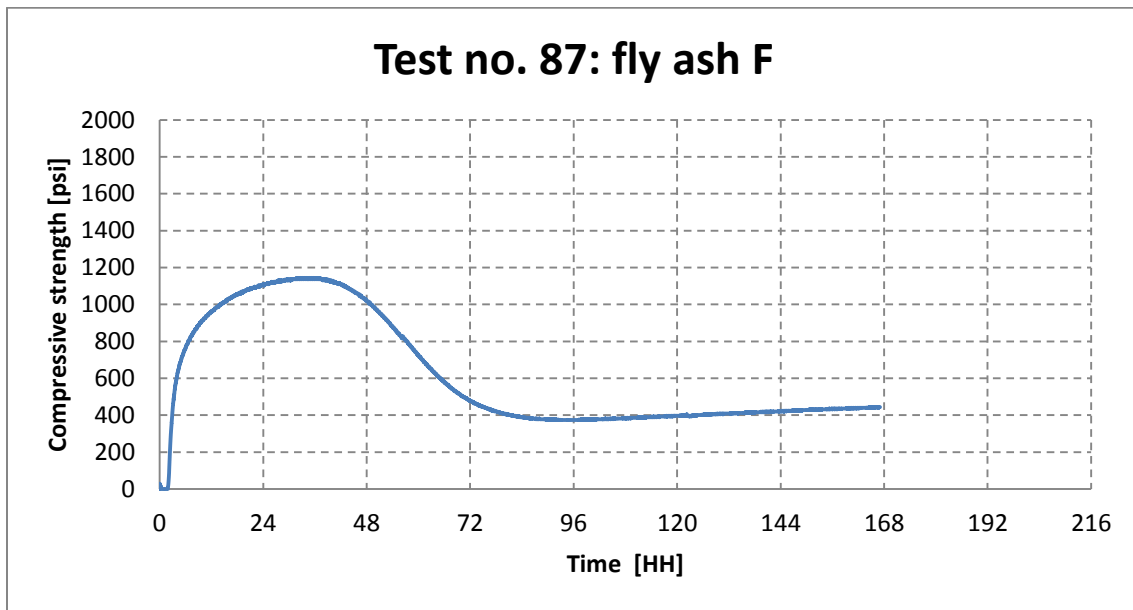


Figure 6.7: Graphical presentation of the result from the UCA test of sample no. 87. Performed at a curing pressure of 5100 psi and curing temperature of 88°C.

Table 6.8: Key features from the original graph are tabulated in Appendix A, for test no. 87.

| | Strength (psi) | Transit time (ms/in) | Temperature (°C) | Time (HH:MM) |
|-----------------------------|----------------|----------------------|------------------|--------------|
| 50 psi | 50 | 11.7 | 90 | 2:05 |
| 500 psi | 500 | 10.7 | 89 | 3:18 |
| Max strength | 1144 | 9.8 | 88 | 32:35 |
| Reached curing temp. (88°C) | 15 | 11.8 | 88 | 1:57 |
| End point | 444 | 10.8 | 89 | 167:02 |

Test number 100

A graphical presentation of the compressive strength in psi as function of time is shown in Fig. 6.8. The key features from the original graph are tabulated in Appendix A, is shown in Table 6.9.

The test lasted approximately 162 hours. The onset time of the strength was after approximately 2 hours. There was first a rapid buildup of the strength, before the rate of the buildup decreased. The strength reached its highest point at 1191 psi after 112 hours and was quite stable hereafter. However, at the end of the test there was a small decrease and when the test ended, after approximately 162 hours, the strength was 1153 psi and still decreasing.

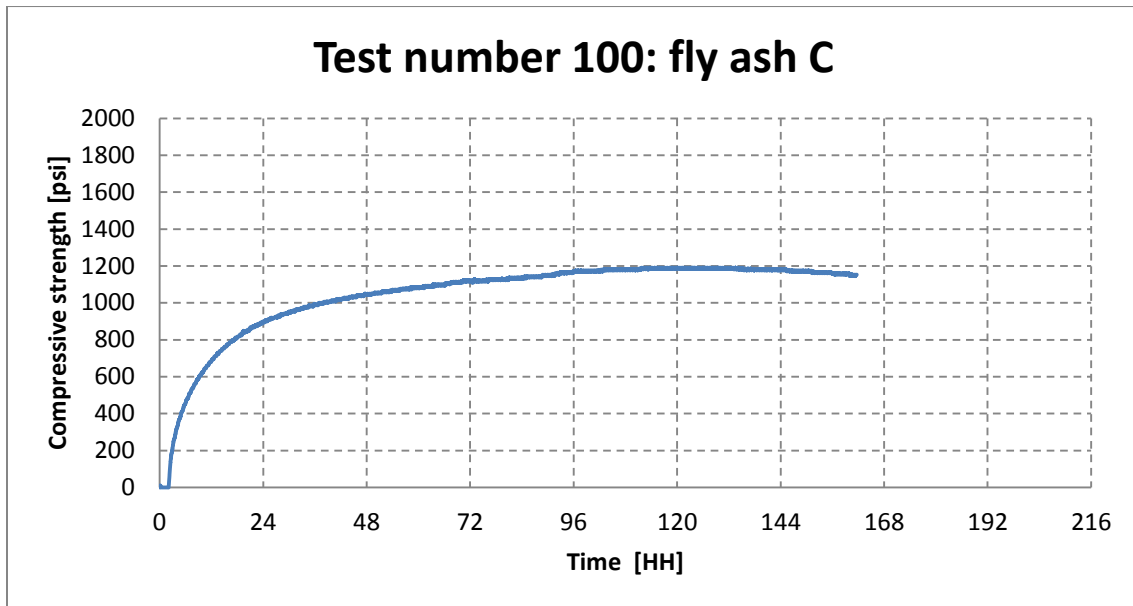


Figure 6.8: Graphical presentation of the result from the UCA test of sample no. 100. Performed at a curing pressure of 5100 psi and curing temperature of 88°C.

Table 6.9: Key features from the original graph are tabulated in Appendix A, for test no. 100.

| | Strength (psi) | Transit time (ms/in) | Temperature (°C) | Time (HH:MM) |
|------------------------------------|-------------------|-------------------------|---------------------|-----------------|
| 50 psi | 50 | 11.3 | 91 | 2:14 |
| 500 psi | 500 | 10.4 | 88 | 6:45 |
| Max strength | 1191 | 9.6 | 88 | 111:49 |
| Reached curing temp. (88°C) | 0 | 11.5 | 88 | 1:57 |
| End point | 1153 | 9.6 | 89 | 161:39 |

Test number 130

A graphical presentation of the compressive strength in psi as function of time is shown in Fig. 6.9. The key features from the original graph are tabulated in Appendix A, is shown in Table 6.10.

The test lasted approximately 163 hours. The onset time for the compressive strength was approximately 2 hours. There was first a rapid buildup of the strength, before the rate of the buildup rate decreased. However, the compressive strength continued to increase and when the test ended after approximately 163 hours, the compressive strength was 1860 psi, still increasing.

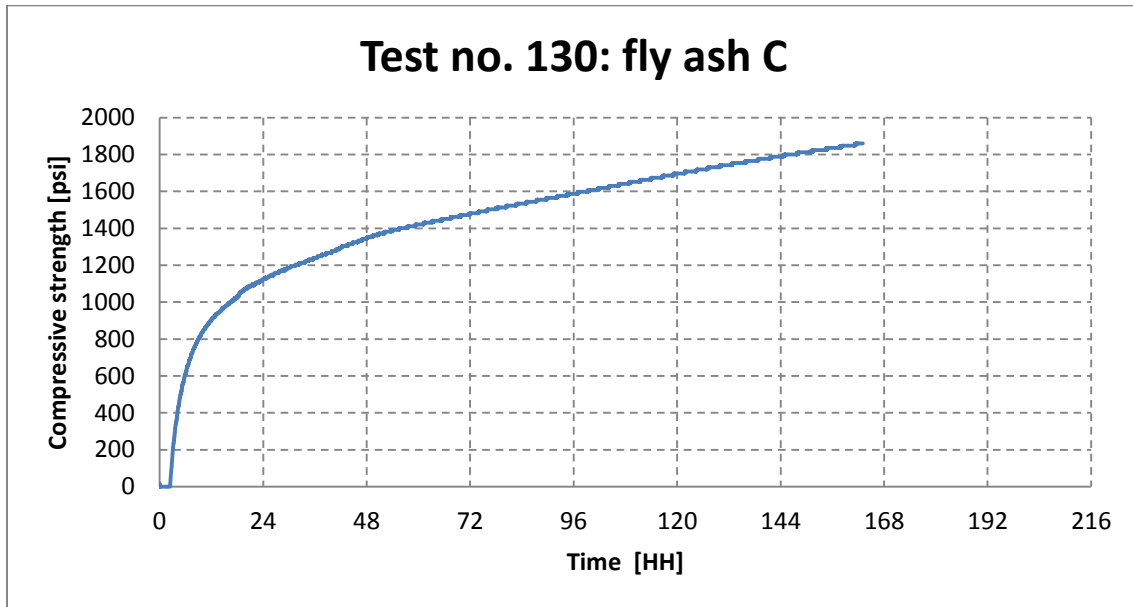


Figure 6.9: Graphical presentation of the result from the UCA test of sample no. 130. Performed at a curing pressure of 5100 psi and curing temperature of 88°C.

Table 6.10: Key features from the original graph are tabulated in Appendix A, for test no. 130.

| | Strength (psi) | Transit time (ms/in) | Temperature (°C) | Time (HH:MM) |
|------------------------------------|-------------------|-------------------------|---------------------|-----------------|
| 50 psi | 50 | 10.7 | 88 | 02:33 |
| 500 psi | 500 | 10.1 | 89 | 04:50 |
| Max strength | 1860 | 8.9 | 89 | 161:33 |
| Reached curing temp. (88°C) | 0 | 11.5 | 88 | 01:52 |
| End point | 1860 | 8.9 | 88 | 163:03 |

6.4.2. Uniaxial Compressive Strength tests

A total of eleven samples were prepared during this experimental work, using the same materials as in test no. 130 from the UCA test. Eight of these samples were prepared at high pressure and at high temperature. The temperature was 87°C and the pressure was approximately 1300 psi. The last four samples were prepared at atmospheric pressure and at room temperature. After mixing the materials in regard to the recipes, the geopolymer plugs were molded in cylindrical plastic containers for seven days. Afterwards the samples were cut and prepared for the UCS tests.

The original graphs from the UCS tests are presented in Appendix B. It should be noted that in this text the maximum applied force from the original graphs are converted from kilo Newton (kN) to compressive strength in psi by dividing the force by the area of the sample.

6.4.2.1. Recipes

Three different recipes were used during this experiment. It should be noted that for each of the recipes presented in the next section, the SLR was kept constant at 2.1. The recipes differ in the NaOH concentration; they vary between 6M, 8M and 10M NaOH.

Test number 115 A-G

The recipes of sample no. 115 A-G are presented in Table 6.11. A 8M NaOH concentration was used in this recipe. Sample 115 A-C were prepared at high pressure and high temperature, while sample 115 D-G were prepared at atmospheric pressure and room temperature.

Table 6.11: Recipes of sample 115 A-G.

| Test number | Fly ash C (g) | Water glass (g) | 8M NaOH (g) |
|--------------------|----------------------|------------------------|--------------------|
| 115 A | 369.2 | 87.8 | 87.8 |
| 115 B | 369.2 | 87.8 | 87.8 |
| 115 C | 369.1 | 87.8 | 87.8 |
| 115 D | 371.3 | 87.8 | 87.8 |
| 115 E | 369.2 | 87.8 | 87.8 |
| 115 F | 369.1 | 87.8 | 87.8 |
| 115 G | 369.7 | 87.8 | 87.7 |

Test number 131 A and B

The recipes of sample no. 131 A and B are presented in Table 6.12. A 6M NaOH concentration was used in this recipe. The samples were prepared at high pressure and high temperature.

Table 6.12: Recipes of sample 131 A and B.

| Test number | Fly ash C (g) | Water glass (g) | 6 M NaOH (g) |
|-------------|---------------|-----------------|--------------|
| 131 A | 369.2 | 87.8 | 87.8 |
| 131 B | 369.2 | 87.8 | 87.8 |

Test number 132 A and B

The recipes of sample no. 132 A and B are presented in Table 6.13. A 10M NaOH concentration was used in this recipe. The samples were prepared at high pressure and high temperature.

Table 6.13: Recipes of sample 132 A and B.

| Test number | Fly ash C (g) | Water glass (g) | 10 M NaOH (g) |
|-------------|---------------|-----------------|---------------|
| 132 A | 554.0 | 131.7 | 131.7 |
| 132 B | 554.0 | 131.7 | 131.7 |

6.4.2.2. Results

Test number 115

When sample 115 D, 115 E and 115 F had cured for seven days, it had still not set. The lid on top of the samples was removed to see if this would affect the setting properties of the samples. The samples cured for seven more days, but unfortunately they had still not set. It was possible to scratch the sample with a fingernail, indicating that the sample had still not set properly. Both sample 115 D and 115 E had cracked throughout the sample. Two pictures of sample 115 D showing the crack can be seen in Fig. 6.10.

Therefore a new sample, 115 G, was prepared. During the curing time of sample 115 G a lid was not used. After seven days, sample 115 G showed similar conditions as for sample 115 D-F. Sample 115 G was soft and had not set properly. Due to the poor setting of the samples 115 D-G, there were not conducted any UCS tests on these samples.



Figure 6.10: Sample no. 115 D showing a clear crack throughout the sample

The test results from the UCS test are presented in Table 6.12. It should be noted that when performing the UCS test on sample no. 115 A the sample was not centered in the UCS, so the results is not accurate. The average compressive strength is therefore calculated based on the results from test no. 115 B and 115 C. The average compressive strength was found to be 8408 psi. It should be noted that the length of the samples varied which will affect the strength of the samples.

Table 6.14: Results for test no. 115 A-G from the UCS tests.

| Test number | Diameter (mm) | Length (mm) | Compressive strength (psi) |
|-------------|---------------|-------------|----------------------------|
| 115 A | 52.0 | 92.0 | 3150 |
| 115 B | 52.0 | 89.0 | 8671 |
| 115 C | 52.0 | 87.0 | 8147 |

Scanning Electron Microscope (SEM) images were taken of samples 115 B and 115 C subsequent of UCS tests. Both samples showed similar texture. For instance, taken SEM images of sample 115 B are shown in Figs. 6.11, 6.12 and 6.13. Fig. 6.11 has a magnitude of 1000 and it clearly shows circular particles which are fly ash particles that have not reacted with the alkali solution. There can also be seen amorphous parts in Fig. 6.11. Fig. 6.12 shows a closer picture of one of the amorphous parts, a magnitude of 10 000. The amorphous parts is a good indicator that geopolymerization has occurred. An even closer look at another part of the sample, a magnitude of 50 000, showed an unspecified particle area. This is shown in Fig. 6.13.

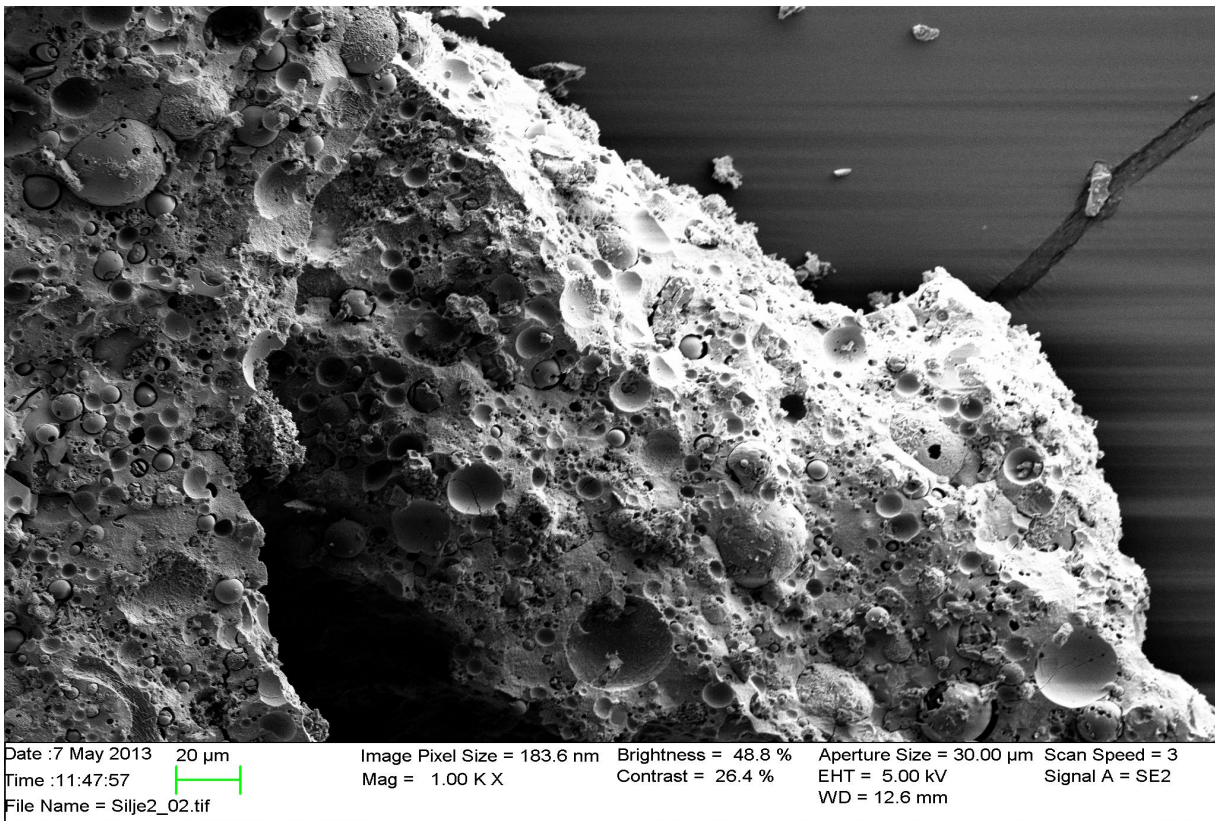


Figure 6.11: SEM image of sample 115 B with a magnitude of 1000. Showing circular particles which are fly ash particles that have not reacted with the alkali solution.

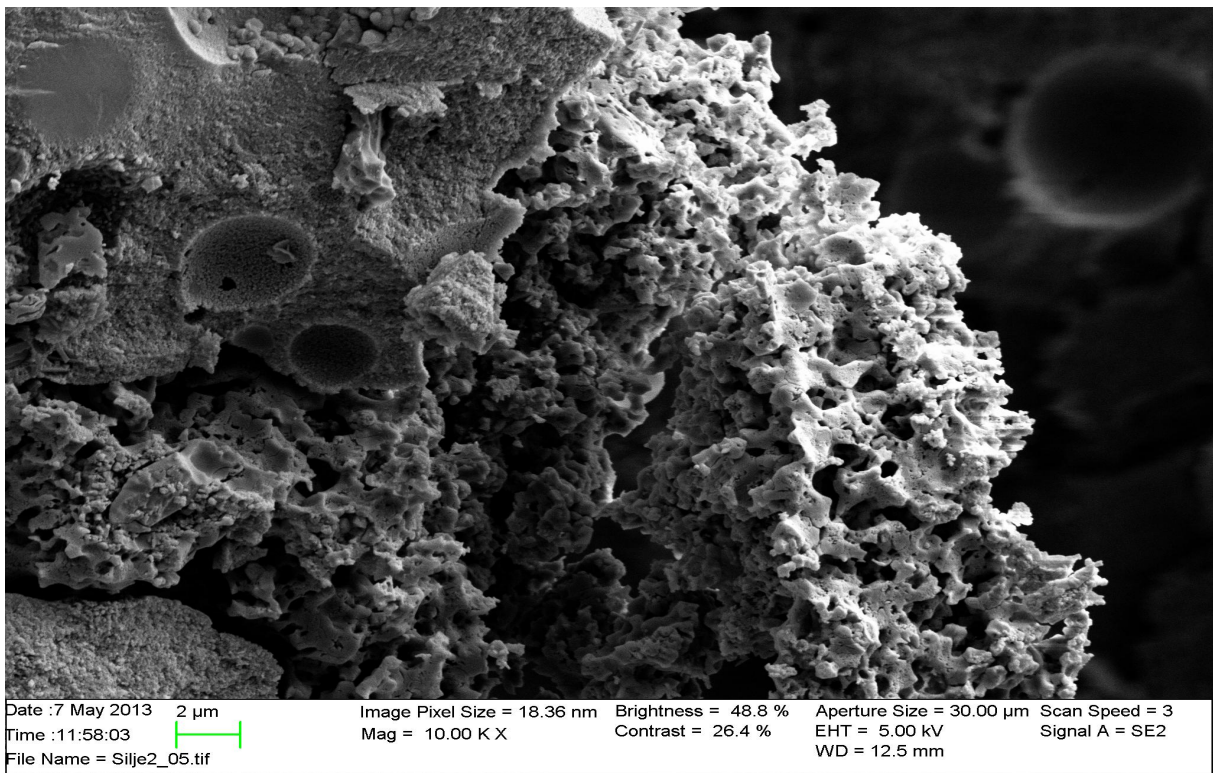


Figure 6.12: SEM image of sample 115 B with a magnitude of 10 000. Showing an amorphous area of the sample.

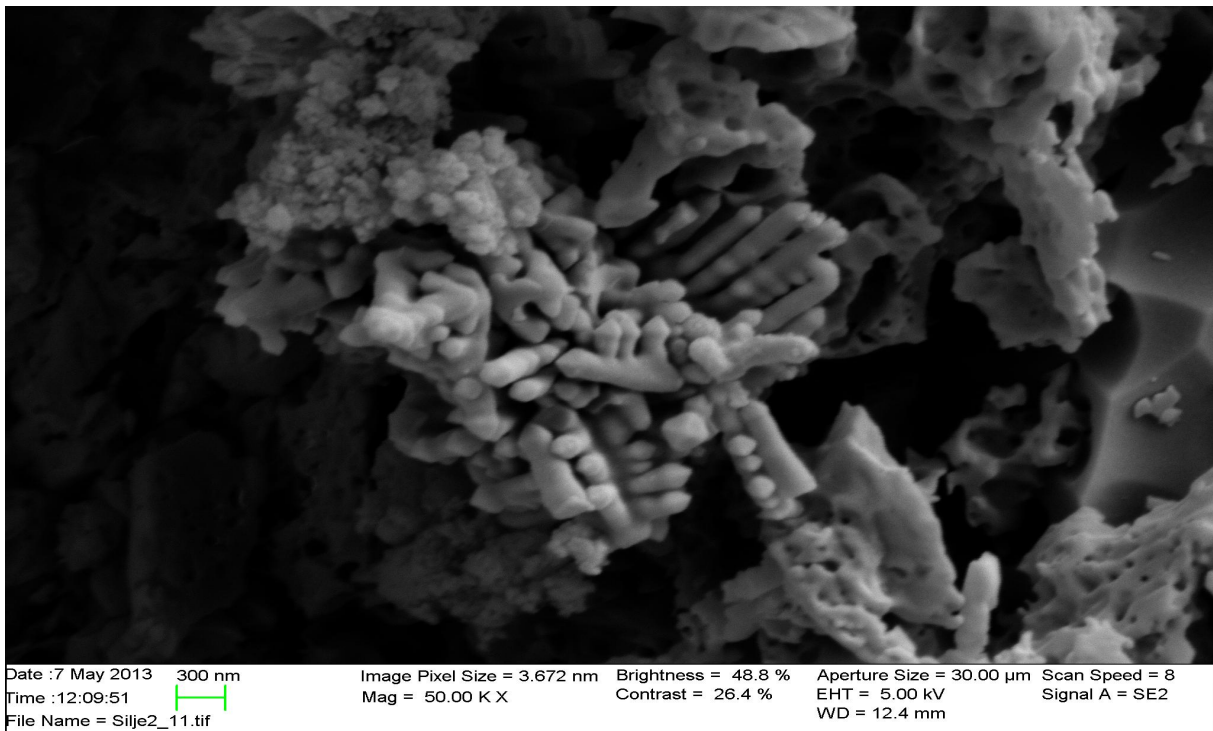


Figure 6.13: SEM image of sample 115 D with a magnitude of 50 000. Showing an unspecified area of the sample.

Test number 131 A and B

The test results from the UCS test are presented in Table 6.15. The average compressive strength was calculated to 5609 psi. Due to the fact that the samples are equal in length makes the results more reliable and provides a better basis for comparison of the two samples.

Table 6.15: Results for test no. 131 A and B from the UCS test.

| Test number | Diameter (mm) | Length (mm) | Compressive strength (psi) |
|--------------------|----------------------|--------------------|-----------------------------------|
| 131 A | 52.0 | 87.0 | 5678 |
| 131 B | 52.0 | 87.0 | 5539 |

Test number 132 A and B

The test results from the UCS test are presented in Table 6.16. The average compressive strength was calculated to 9107 psi. As for sample no. 131 A and B, the samples are equal in length, making the results more reliable and providing a better basis for comparison of the two samples.

Table 6.16: Results for test no. 132 A and B from the UCS test.

| Test number | Diameter (mm) | Length (mm) | Compressive strength (psi) |
|--------------------|----------------------|--------------------|-----------------------------------|
| 132 A | 52.0 | 87.0 | 7629 |
| 132 B | 52.0 | 87.0 | 10 584 |

6.5. Discussion

6.5.1. Comparison of the Ultrasonic Cement Analyzer results

In this section obtained UCA results will be compared and presented in figures where compressive strength is plotted in psi vs. time in hours. It should be noted that due to technical difficulty in test no. 84, this test will not be presented. For details about the material compositions of the test, see Ch. 6.4.1.1 (Recipes).

6.5.1.1. Test number 58 vs. 62

In Fig. 6.15 the upper blue and the lower red curves present collected data from test no. 58 and no. 62, respectively. Test no. 58 and test no. 62 achieved maximum compressive strength of 1958 psi and 1684 psi, respectively. In test no. 62, MK-750 was removed. Hence, it might be said that the MK-750 has a constructive effect on the buildup of compressive strength. According to the literature reviews MK-750 can increase the final compressive strength. So, the amount of MK-750 should be optimized.

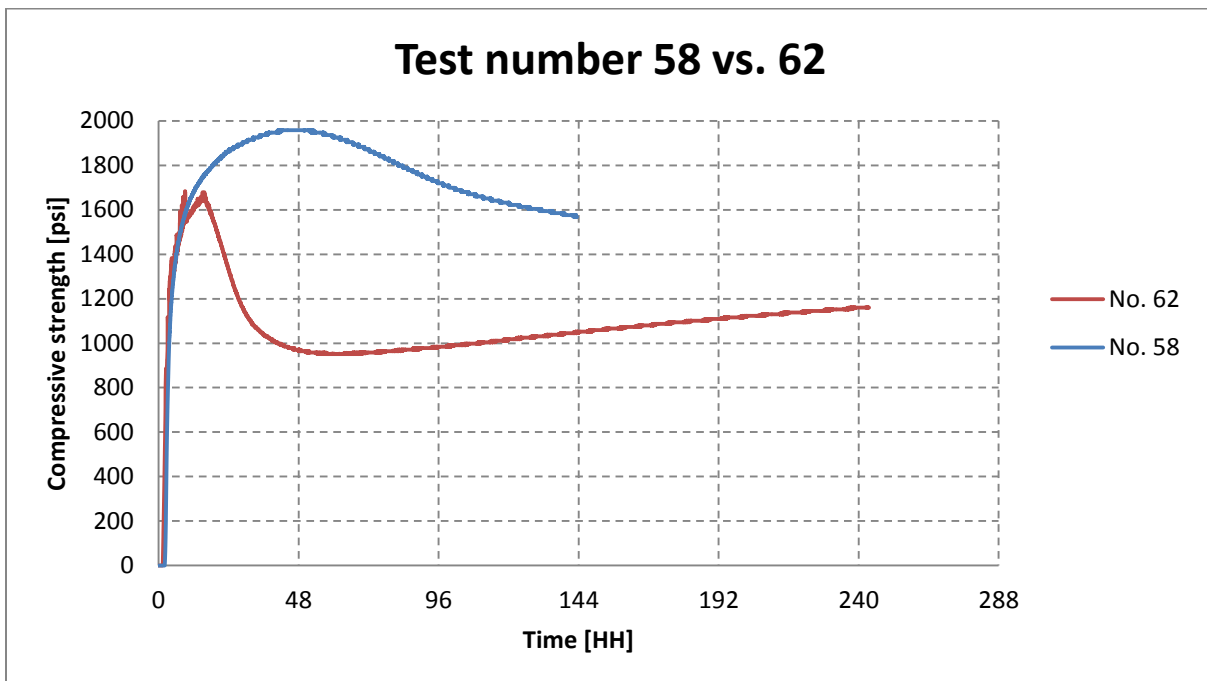


Figure 6.14: Figure illustrates the effect of removing MK-750 content in no. 62 on the compressive strength. Performed at a curing pressure of 5100 psi and curing temperature of 88°C.

6.5.1.2. Test number 58 vs. 76

In Fig. 6.15 the upper red curve presents collected data from test no. 76 and the lower blue curve presents data for test no. 58. In test no. 76 the amount of MK-750, 8M NaOH and water glass was increased. It should be noted, in order to keep the solid-liquid ratio constant the amount of liquid solution was also increased. However, higher liquid content was necessary because of high viscosity of slurry which was due to high surface area of MK-750. The maximum compressive strength in test no. 76 was found to be 1990 psi, so there was only a small increase in the strength compared to no. 58 that reached 1958 psi. Even though the maximum strength was quite similar, the final strength of test no. 76 was higher and the slope of the curve was lower than for the obtained data for test no. 58. The increased compressive strength might be effect of the increased amount of MK-750. Since the strength was increased, it was concluded that this test should be repeated with higher amount of MK-750.

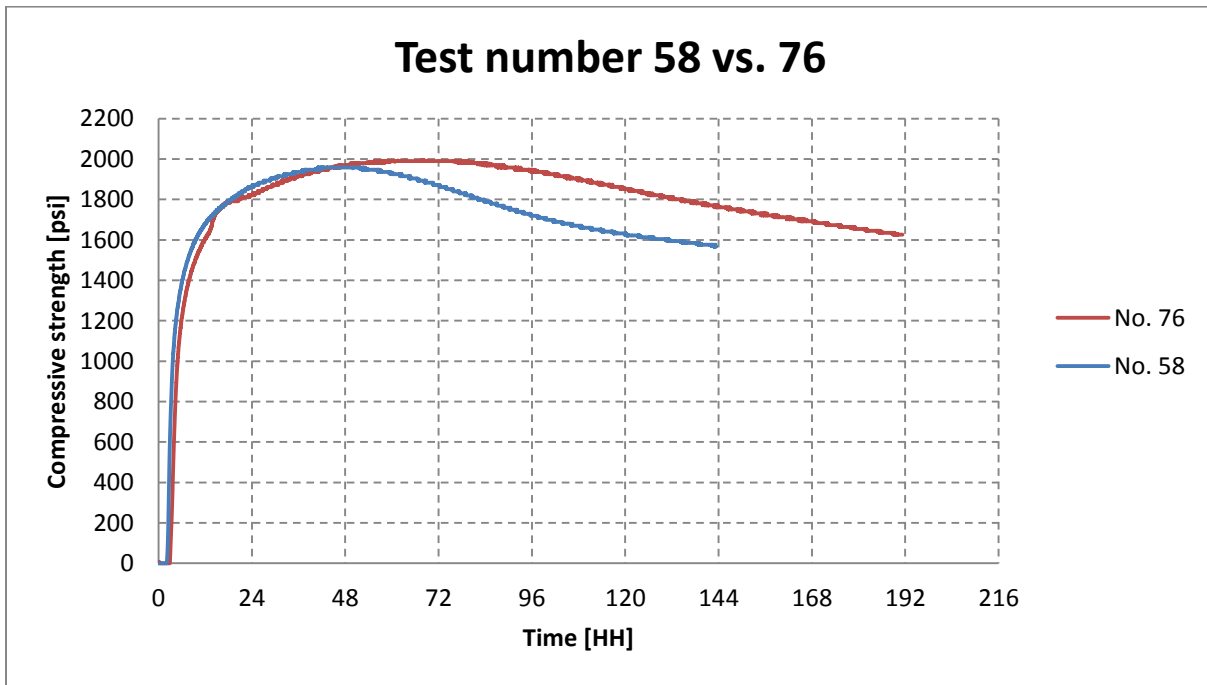


Figure 6.15: Figure illustrates the effect of increased amount of MK-750, water glass and 8M NaOH in no. 76. Performed at curing pressure of 5100 psi and curing temperature of 88°C.

6.5.1.3. Test number 76 vs. 87

In Fig. 6.16 the upper blue and lower red curves present the obtained data from tests no. 76 and 87, respectively. The amount of MK-750, water glass and 8M NaOH was increased and the amount of silica was decreased in test no. 87. Since the silicate-aluminate ratio is the dominant parameter of geopolymerization process, MK-750 content was increased which is a source of silica and aluminum. Moreover, in order to make an economical material the quartz content was decreased. Whereof MK-750 has high surface area by increasing its content, the liquid content should be increased to reduce the viscosity and stir the slurry. The maximum compressive strength for tests no. 87 and 76 were 1144 psi and 1990 psi, respectively. The result from test no. 87 was significantly lower than the obtained result from test no. 76. This could indicate that the amount of silica was too low which caused reduction of compressive strength.

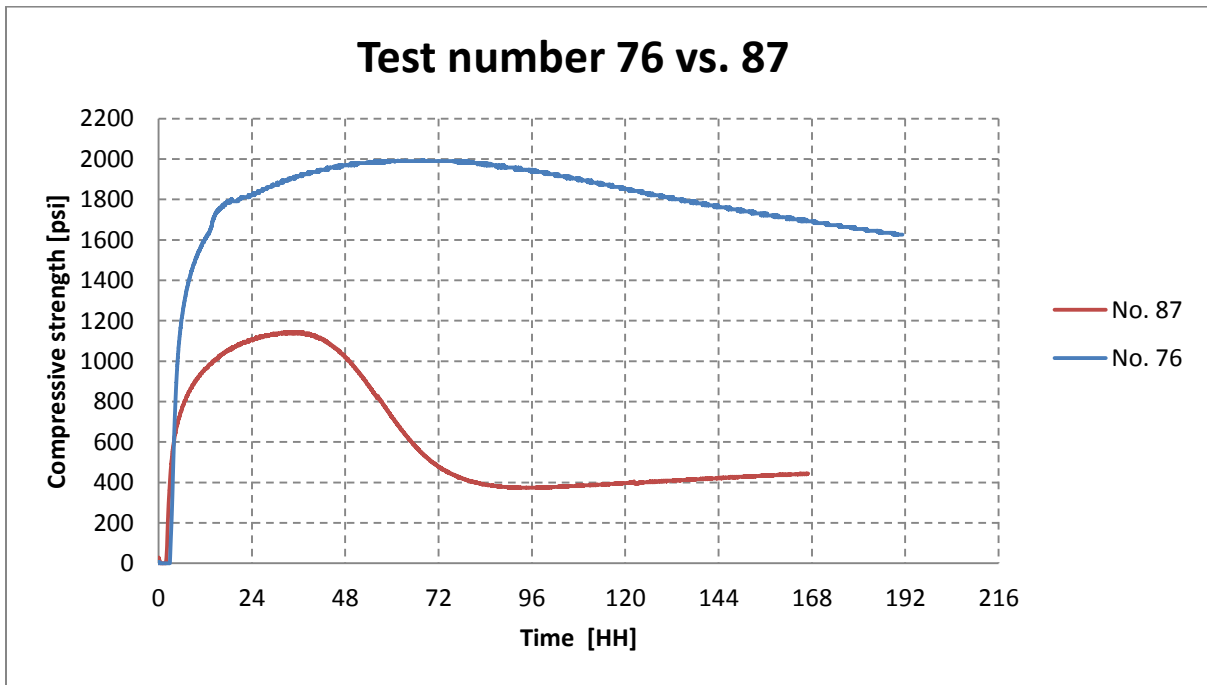


Figure 6.16: Figure illustrated the effect of increased amount of MK-750, 8M NaOH and water glass and decreased amount of silica in no. 87. Performed at curing pressure of 5100 psi and curing temperature of 88°C.

6.5.1.4. Test number 76 vs. 100

A new recipe was used in test no. 100 where the amount of 8M NaOH was increased and the amount of water glass was decreased. In Fig. 6.17 the upper blue curve presents results for test no. 76 while the lower red curve presents results for test no. 100. The maximum compressive strength in no. 76 was found to be 1990 psi while for test no. 100 it was 1191 psi. The decreased amount of water glass could be the reason for the lowered compressive strength due to lower silica content.

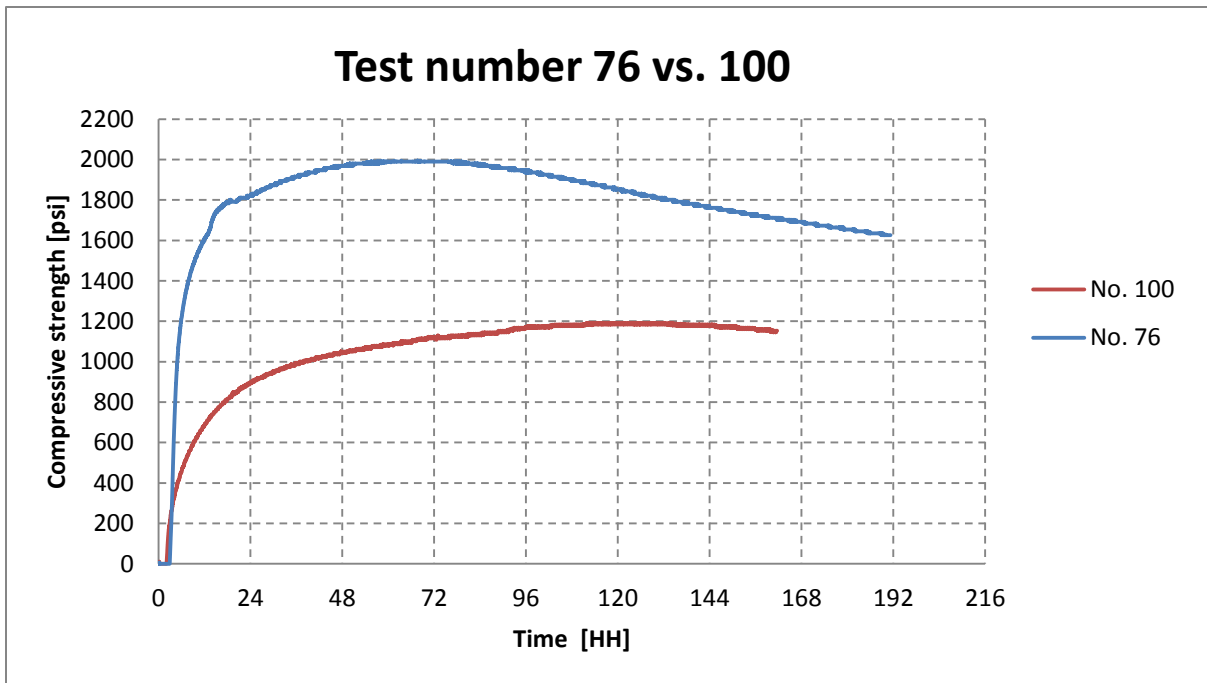


Figure 6.17: Figure illustrates the effect of increased amount of 8M NaOH and decreased amount of water glass content in no. 100. Performed at a curing pressure of 5100 psi and a curing temperature of 88°C.

6.5.1.5. Test number 100 vs. 130

In Fig. 6.18 the upper blue and lower red curves present the obtained data from tests no. 130 and 100, respectively. In test no. 130 the MK-750, silica and BFS were removed. The maximum compressive strength in no. 100 was found to be 1191 psi while for test no. 130 it was 1860 psi. The strength in test no. 130 was still increasing when the test stopped, meaning that the strength would be even higher if the test had continued. This could indicate that the removal of MK-750, silica and BFS has a positive effect on the strength development.

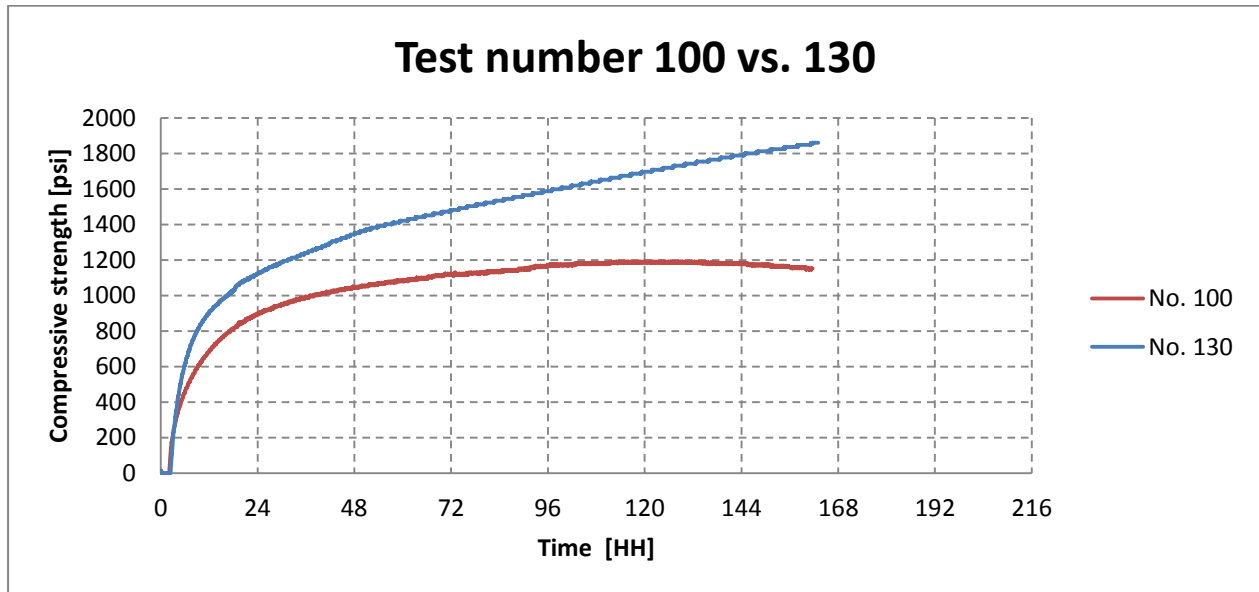


Figure 6.18: Figure illustrates the effect of removing MK-750, silica and BFS in no. 130. Performed at a curing pressure of 5100 psi and a curing temperature of 88°C.

6.5.2. Comparison of the UCA and UCS results

The obtained UCA results from test no. 130 was compared with the obtained UCS results for tests no. 115 B and C, 131 A and B and 132 A and B. The compressive strength results from the UCA and UCS tests are presented in Table. 6.17.

Table 6.17: Results from the UCS tests

| Test number | Compressive strength (psi) | Average compressive strength (psi) |
|-------------|----------------------------|------------------------------------|
| 115 B | 8671 | 8408 |
| 115 C | 8145 | |
| 131 A | 5678 | 5609 |
| 131 B | 5539 | |
| 132 A | 7629 | 9107 |
| 132 B | 10 584 | |

The compressive strength was significantly higher in the UCS tests than in the UCA test no. 130, which was found to be 1860 psi. However, it should be noted that the strength in the UCS tests may vary due to different lengths of the geopolymer plugs. It should also be noted that the strength development in the UCA test no. 130 was increasing at all times, indicating that the strength could be significantly higher if the test had continued. However, it could take several days before the strength approached the strength found in the UCS tests, if it ever would.

It was also found from the UCS tests that a higher NaOH concentration increased the maximum compressive strength of the geopolymer plugs. This may indicate that there has occurred a higher grade of geopolymerization in the slurry when a higher NaOH concentration was present.

It should be mentioned that the UCS results probably are more reliable due to the fact that this is a pure mechanical test. However, both tests should be repeated several times to research if the tests can verify each other better.

6.6. Proposed further work

Since cement is frequently used in high pressure and high temperature wells for P&A operations, it would be essential to investigate the effect of increasing the temperature during the UCA tests of geopolymers. Would a higher temperature have an impact on the compressive strength buildup? Another factor that is essential for cement used in P&A is shrinkage of the cement plug, so this should also be tested for the relevant geopolymer recipe.

There are also several other factors that could be researched further to optimize the recipe and make the geopolymers capable to use in P&A operations. For instance, the geopolymer slurries porosity, permeability, viscosity and bonding conditions could be tested.

The similarity in the UCS tests indicates that the tests were a success. To ensure that the results are correct, several more samples using the same recipe as in these tests should be made and tested in the UCS. Several more samples prepared under atmospheric pressure and in room temperature should be conducted to try to find the reason that they did not set properly.

A last thing that could be recommended for further research is analyzing the impurities that were found in the SEM images. Do these impurities affect the geopolymerization of the sample?

6.7. Conclusion

MK-750 content plays an important role in the compressive development whereas the higher MK-750 content can reduce the compressive strength while low content of MK-750 increases the compressive strength.

Reduced amount of water glass in addition to increased amount of 8M NaOH in the fly ash-based sample used for the UCA test decreased the compressive strength due to lower silica content. Hence, too low silica content in the slurry will decrease the compressive strength due to lower degree of geopolymerization.

Removing every material except fly ash and liquid solutions from the slurry in the UCA test resulted in a positive compressive strength development. The strength was continuously increasing with a high rate, indicating that fly ash and liquid solutions are capable of creating high compressive strength.

The results for developed geopolymers containing only fly ash and liquid solutions revealed a significantly higher maximum compressive strength in the UCS test than in the UCA test. However, this only applies to geopolymers prepared at high pressure and high temperature. For the geopolymer that prepared at room temperature and atmospheric pressure there was not created significant strength.

During the UCS tests for the recipe containing only fly ash and liquid solutions it was found that a higher NaOH concentration increased the maximum compressive strength.

7. References

- [1] Smith D. K., 1993. *Handbook on well plugging and abandonment*. Published by PennWell Books, 1993 ISBN: 0-87814-369-x.
- [2] Talukdar S. and Instefjord R., 2008. *Reservoir Management on the Gullfaks Main Field*. Paper SPE 113260-MS presented at the Europec/EAGE Conference and Exhibition held in Rome, Italy, 9-12 June 2008.
- [3] The Petroleum Safety Authority Norway, 2010. *The Activities Regulations*. Available from: <http://www.ptil.no/activities/category399.html> Visited: 14.01.13.
- [4] NORSOK D-010, 2004. *Well integrity in well and drilling operations. Rev. 3*. Published by Standards Norway, 30 August 2004.
- [5] Khalifeh M., Saasen A., Hodne H. and Vrålstad T., 2013. *Techniques and Materials for North Sea Plug and Abandonment Operations*. Paper OTC 23915 presented at the Offshore Technology Conference held in Huston, Texas, USA 6-9 May 2013.
- [6] Vignes, B. and B.S. Aadnoy, 2008. *Well-Integrity Issues Offshore Norway*. Paper SPE/IADC 112535 presented at the SPE/IADC Drilling Conference held in Orlando, Florida, USA 4-6 March 2008.
- [7] Oil & Gas United Kingdom, 2011. *Guideline on Well Abandonment Cost Estimation, Issue 1*. Published by Oil & Gas UK, April 2011. ISBN: 1 903 003 69 3.
- [8] Oil & Gas United Kingdom, 2012. *Guidelines for the suspension and abandonment of well, Issue 4*. Published by Oil & Gas UK, July 2012. ISBN: 1 903 003 84 2.
- [9] Oil & Gas United Kingdom, 2012. *Guidelines of qualification of materials for the suspension and abandonment of wells: issue 1*. Published by Oil & Gas UK, July 2012. ISBN: 1 903 003 85 4.
- [10] Ferg T. E., Lund H. J., Mueller D. T., Myhre M., Larsen A. G., Andersen P., Lende G., Hudson C. E., Prestegaard C. and Field D., 2011. *Novel Approach to More Effective Plug and Abandonment Cementing Techniques*. Paper SPE 148640-MS presented at the SPE Arctic and Extreme Environments Conference & Exhibition held in Moscow, Russia 18-20 October 2011.

- [11] Nelson, E.B. and Guillot D., 2006. *Well cementing. 2nd edition*. Published by Schlumberger, 2006. ISBN: 978-097885300-6.
- [12] Wansbrough H., 1998. *The manufacture of Portland cement*. Available from:
<http://nzic.org.nz/ChemProcesses/inorganic/9B.pdf> Visited: 22.01.13.
- [13] Portland Cement Association. *Cement making process*. Available from:
<http://www.cement.org/basics/images/flashtour.html> Visited: 23.01.13.
- [14] Buchwald A., Kaps C. and Hohmann M., *Alkali-activated binders and pozzolan cement binders - complete binder reaction or two sides of the same story?* Available from:
http://www.researchgate.net/publication/228500946_Alkali-activated_binders_and_pozzolan_cement_binderscomplete_binder_reaction_or_two_sides_of_the_same_story Visited: 04.02.13
- [15] The Zeobond Group. *The Geopolymer Solution*. Available from:
<http://www.zeobond.com/geopolymer-solution.html> Visited: 13.02.13.
- [16] Khale D. and Chaudhary R., 2005. *Mechanism of geopolymerization and factors influencing its development: a review*. DOI: 10.1007/s10853-006-0401-4.
- [17] Davidovits J., 2011. *Geopolymer Chemistry and Applications, 3rd edition*. Published by Institute Gèopolymère, Saint-Quentin, France, July 2011, ISBN: 9782951482050. Available from:
http://www.geopolymer.org/fichiers_pdf/geopolymer-book-chapter1.pdf Visited: 01.03.13.
- [18] Geopolymer Alliance. *The Geopolymerization Process*. Available from:
<http://www.geopolymers.com.au/science/geopolymerization> Visited: 26.04.13.
- [19] Duxson P., Fernández-Jimènes A., Provis J. L., Luckey G. C., Palomo A., and van Deventer J. S. J., 2006. *Geopolymer technology: the current state of art*. DOI: 10.1007/s10853-006-0637-z.
- [20] Rovnaik P., 2009. *Effect of curing temperature on the development of hard structure of metakaolin-based geopolymer*. DOI: 10.1016/j.conbuildmat.2009.12.023.
- [21] Basham K. D., Clark M., France T. and Harrison P., 2007. *Adding Fly Ash to Concrete Mixes for Floor Construction; What is Fly Ash?* Available from:
<http://www.concreteconstruction.net/concrete-construction/adding-fly-ash-to-concrete-mixes-for-floor-constr.aspx> Visited: 10.04.13.

- [22] National Slag Association, 2009. *Blast Furnace Slag: The Construction Material of Choice*. Available from: http://nationalslag.org/archive/nsa_blast_furnace_brochure.pdf Visited: 12.04.13.
- [23] Bezard D. *General description of metakaolin*. Available from: <http://www.metakaolin.info/general-description.html> Visited: 16.04.13.
- [24] Kurtis K.E., 2011. *Benefits of Metakaolin in HPC*. Available from: http://www.bigfreshcontrol.com/documents/act_documents/Metakakaolin_Portion_of_Article.pdf Visited: 16.04.13.
- [25] Britannica Academic Edition. *Water glass*. Available from: <http://www.britannica.com/EBchecked/topic/637082/water-glass> Visited: 17.04.13.
- [26] Orwell M. *What is Silicon Dioxide?* Available from: http://www.ehow.com/about_4600805_what-silicon-dioxide.html Visited: 19.04.13
- [27] Pure solutions. *Silica suppliers*. Available from: <http://www.wmaindia.com/indonesia/silica-powder-exporters.php> Visited: 19.04.13
- [28] Kosmatka S. H., Kerkhoff B. and Panarese W. C., 2002. *Design and Control of Concrete Mixtures, 14th edition*. Published by Portland Cement Association, 2002. ISBN: 0893122173.
- [29] Erwin Z., 2012. *What is NaOH?* Available from: <http://www.qwhatis.com/what-is-naoh/> Visited: 24.01.13
- [30] OFI Testing Equipment, 2011. *Ultrasonic Cement Analyzer, a non-destructive way to determine compressive strength*. Available from: http://www.ofite.com/brochures/120-50_brochure.pdf Visited: 26.03.13
- [31] Forsmark L. J., 2004. M.F. *Uniaxial compression tests*. Available from: <http://www.sp.se/en/index/services/rockmechanicaltesting/uniaxial/Sidor/default.aspx> Visited: 26.03.13

Appendix A

Appendix A contains the original graphs from the Ultrasonic Cement Analyzer (UCA) tests. Each graph shows the time (HH) on the x-axis vs. temperature (°C), transit time (micro sec/in) and compressive strength (psi) on the y-axis.

Test number 58

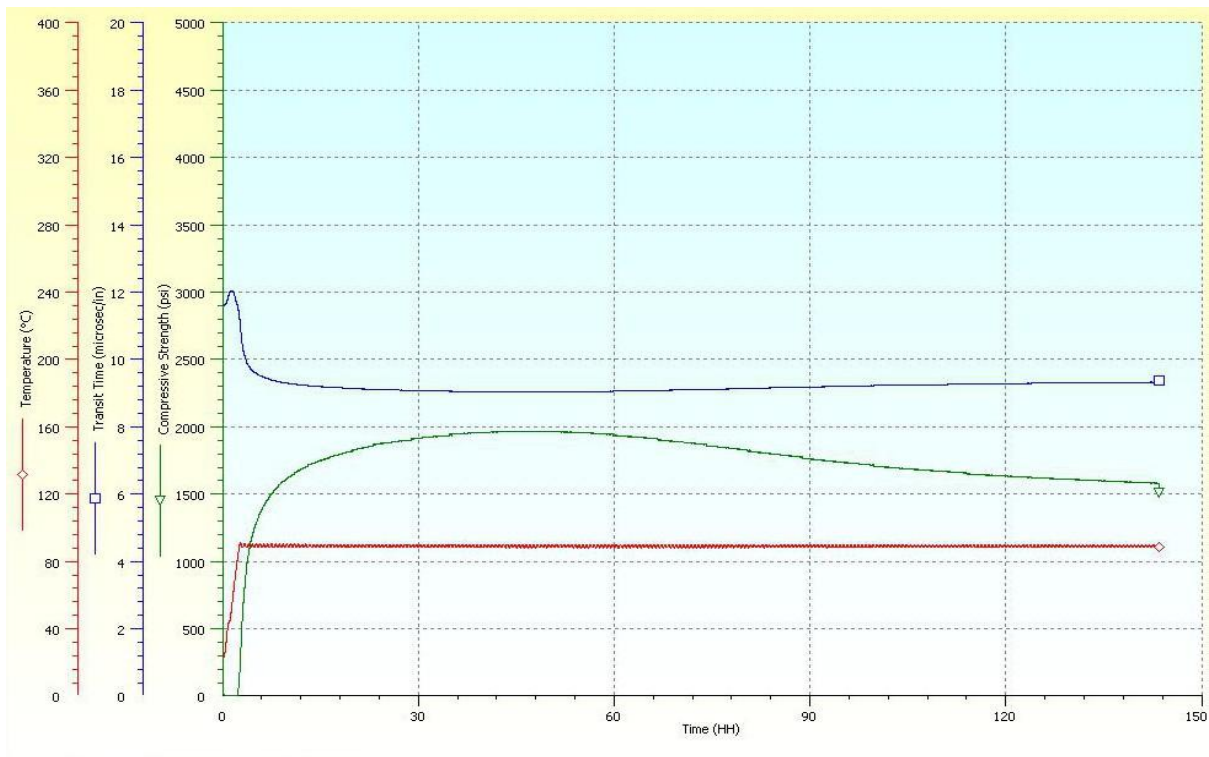


Figure A.1: UCA results for test no. 58. The upper blue curve shows the transit time (micro sec/in), the middle green curve shows the compressive strength (psi) and the lower red curve shows the temperature (°C).

Test number 62

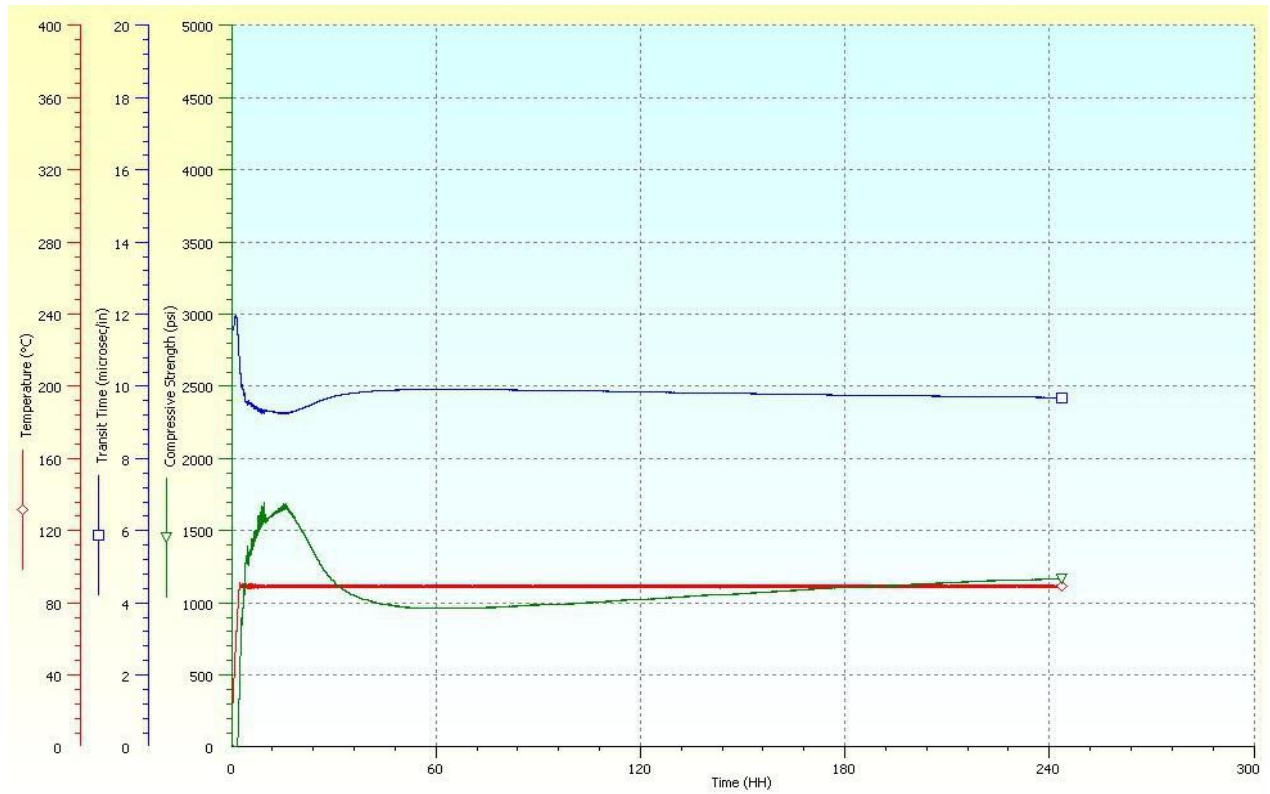


Figure A.2: UCA results for test no. 62. The upper blue curve shows the transit time (micro sec/in), the middle green curve shows the compressive strength (psi) and the lower constant red curve shows the temperature (°C).

Test number 76

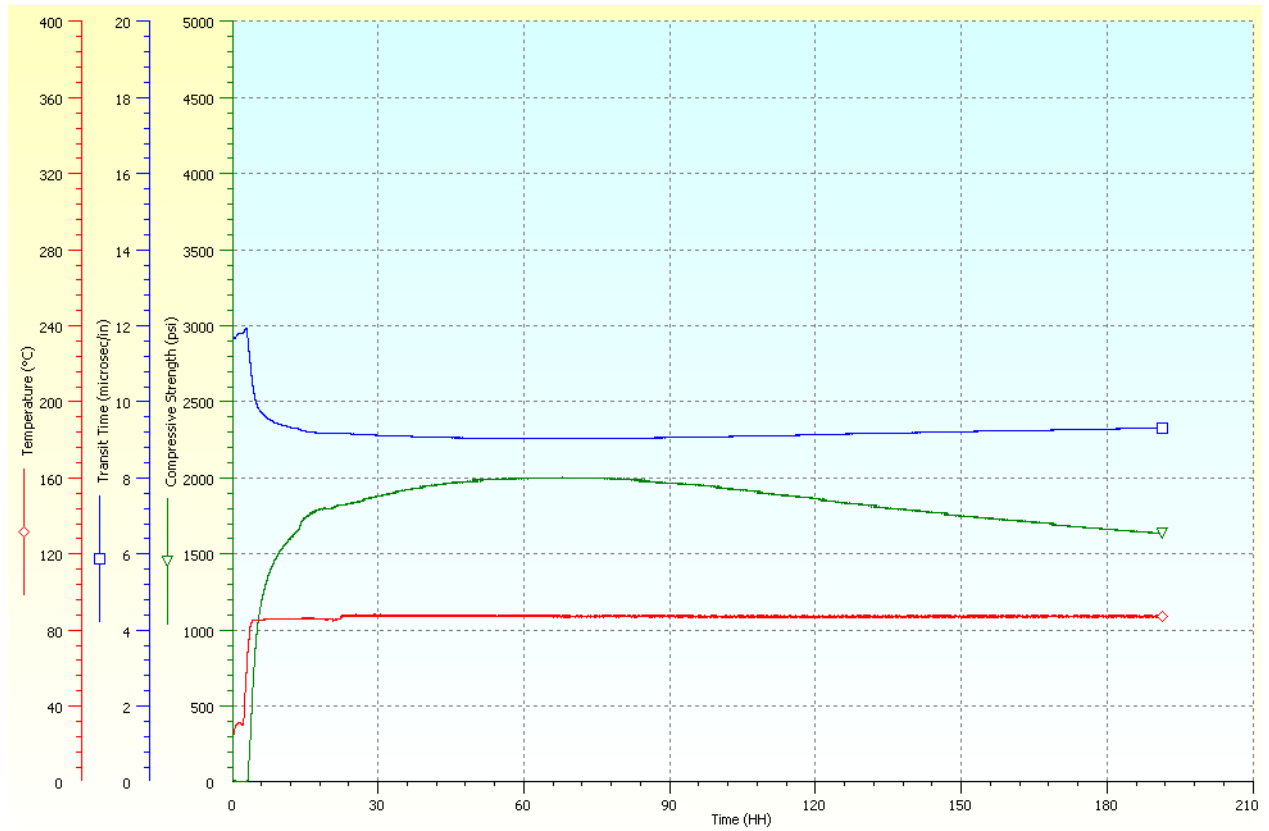


Figure A.3: UCA results for test no. 76. The upper blue curve shows the transit time (micro sec/in), the middle green curve shows the compressive strength (psi) and the lower red curve shows the temperature (°C).

Test number 84

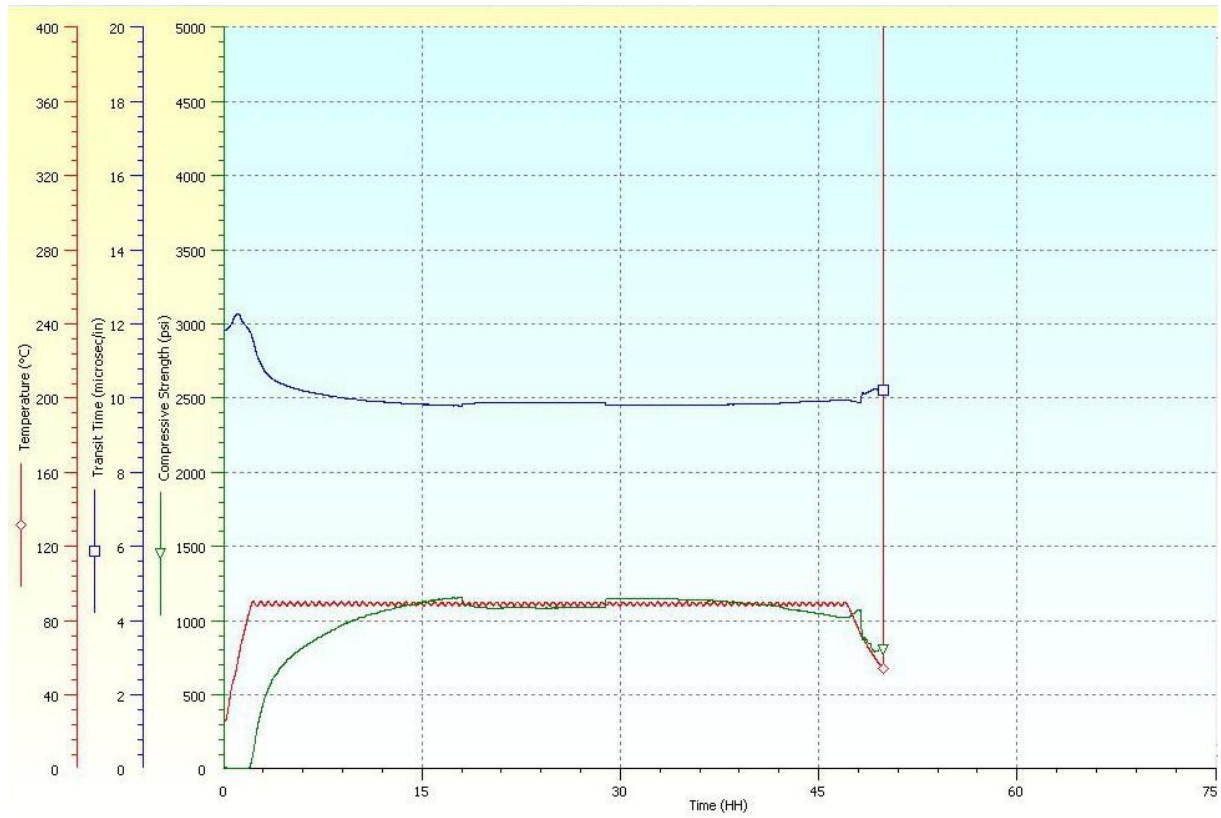


Figure A.4: UCA results for test no. 84. The upper blue curve shows the transit time (micro sec/in), the middle green curve shows the compressive strength (psi) and the lower red curve shows the temperature (°C).

Test number 87

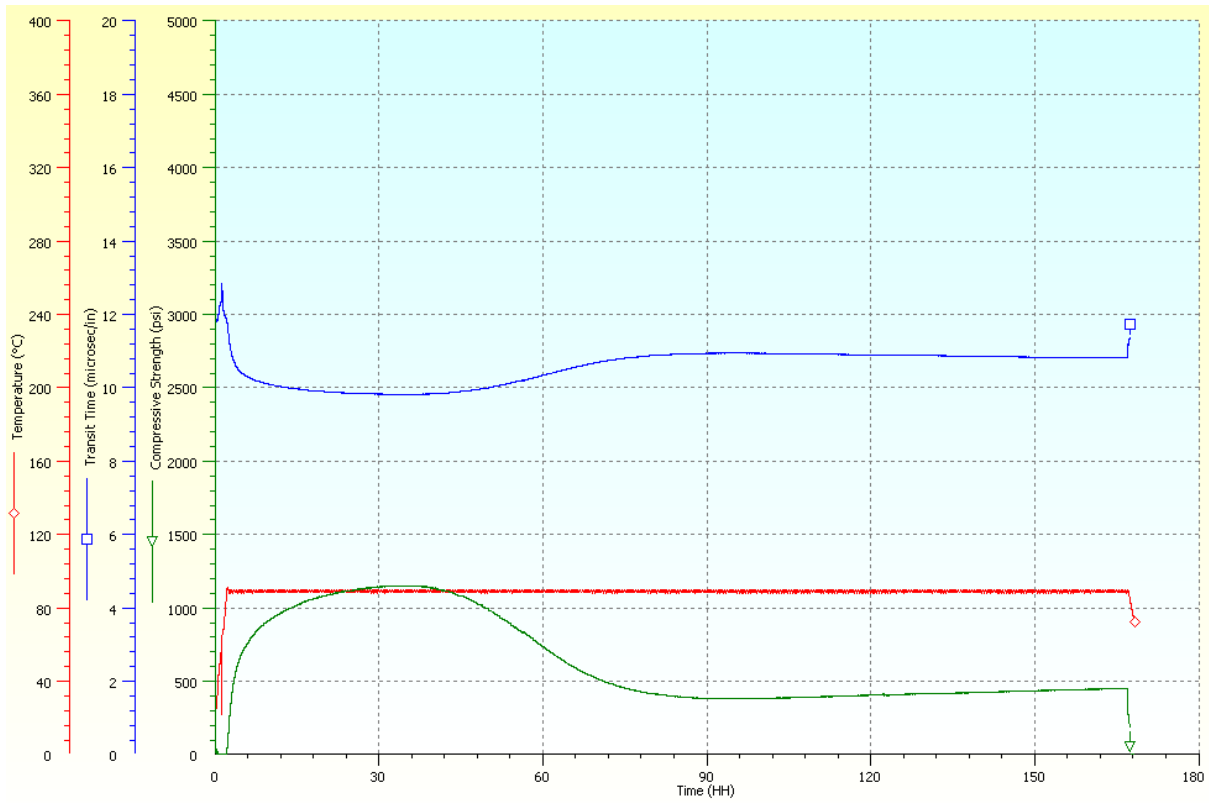


Figure A.5: UCA results for test no. 87. The upper blue curve shows the transit time (micro sec/in), the middle red curve shows the temperature (°C) and the lower green curve shows the compressive strength (psi).

Test number 100

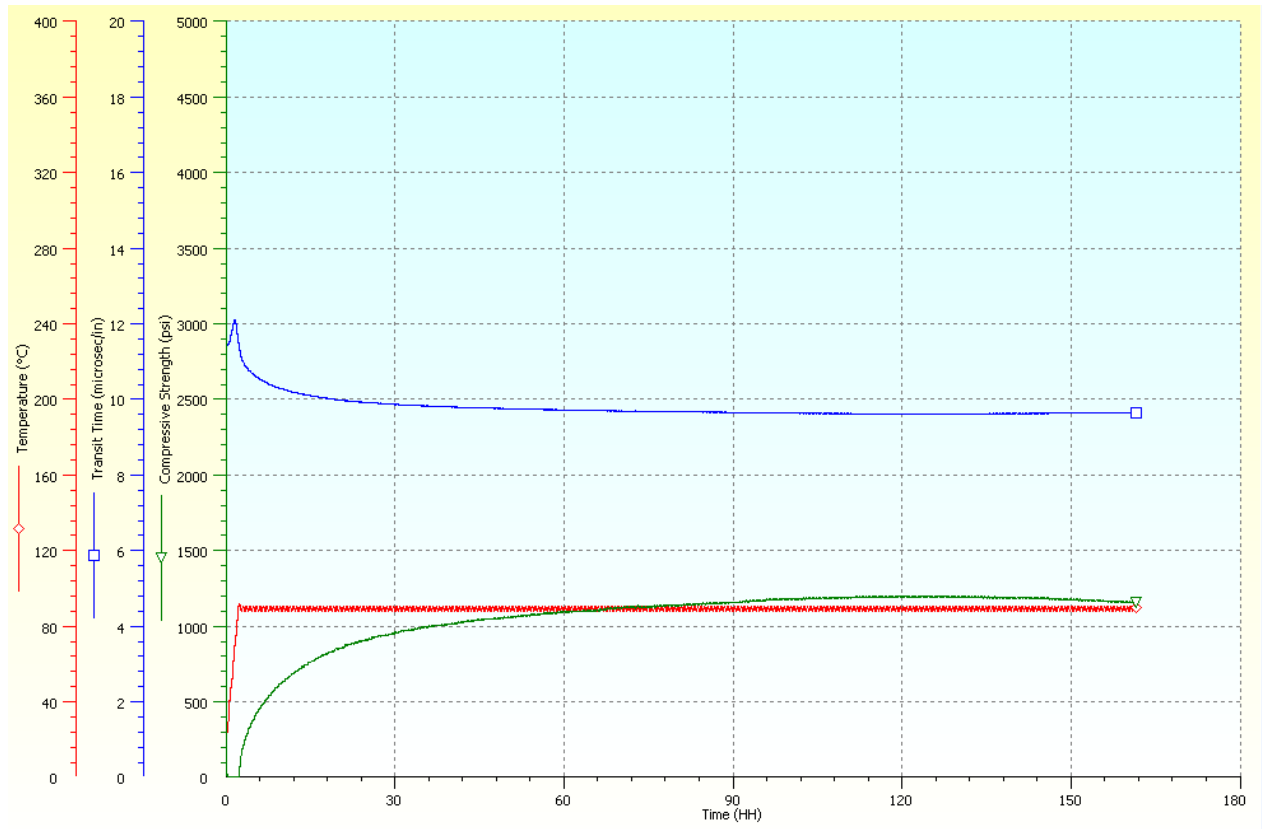


Figure A.6: UCA results for test no. 100. The upper blue curve shows the transit time (micro sec/in), the constant middle red curve shows the temperature (°C) and the lower green curve (crossing the middle red curve at one point) shows the compressive strength (psi).

Test number 130

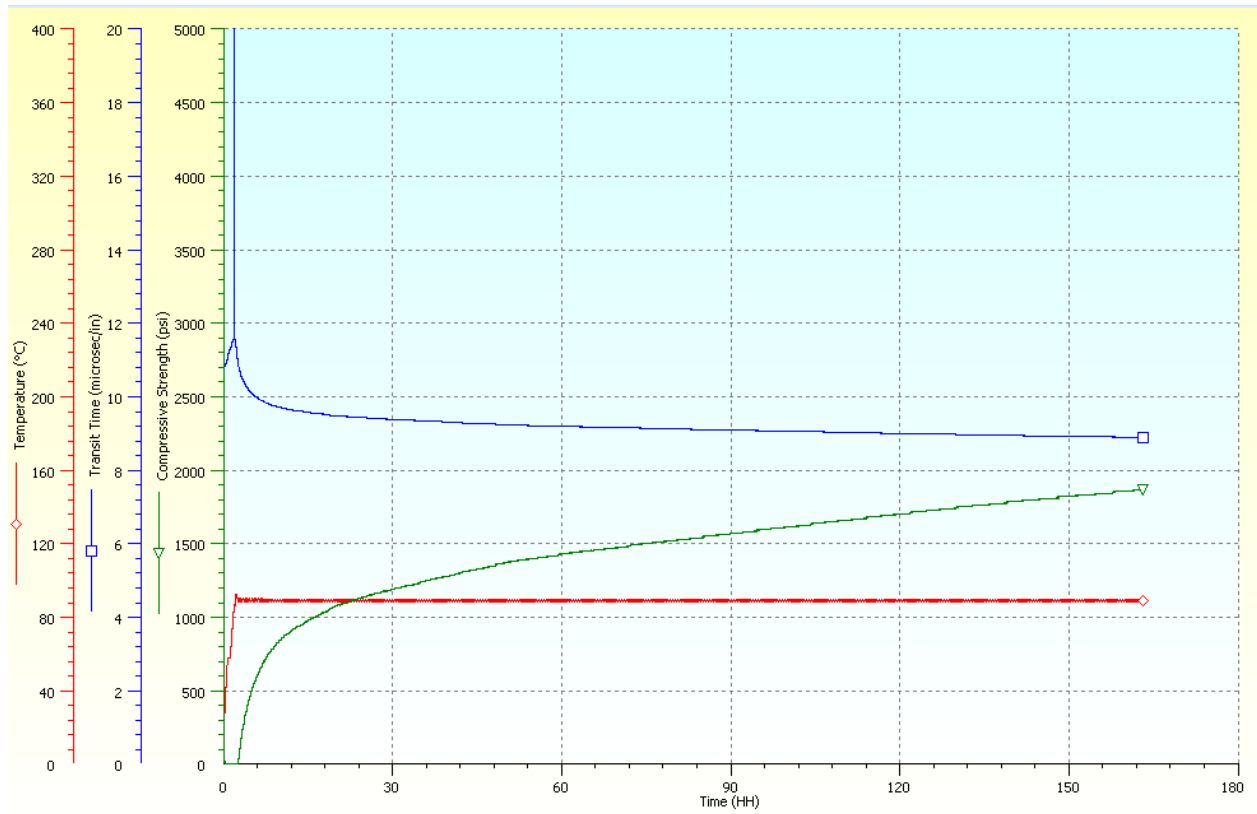


Figure A.7: UCA results for test no. 130. The upper blue curve shows the transit time (micro sec/in), the middle green curve shows the compressive strength (psi) and the lower red curve shows the temperature (°C).

Appendix B

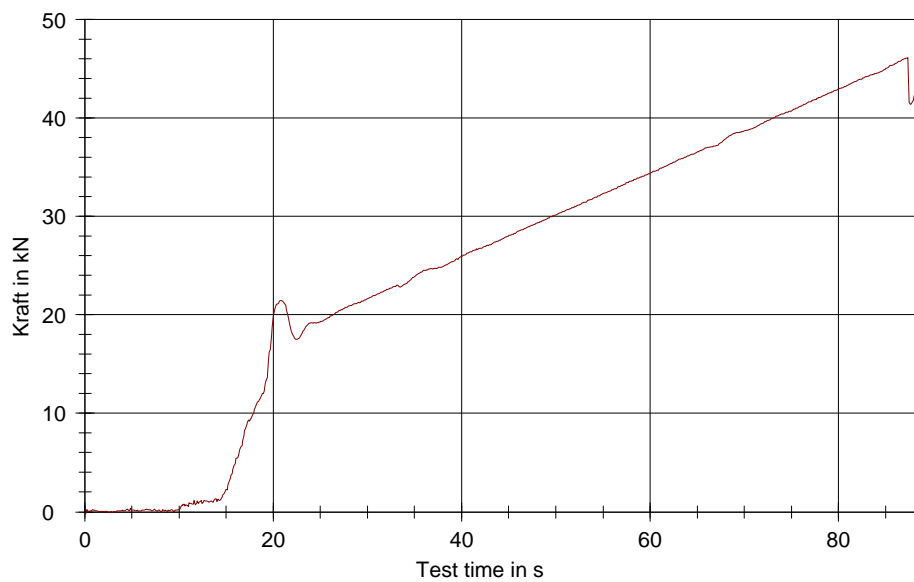
Appendix B contains the original graphs from the Uniaxial Compressive Strength (UCS) tests.

Sample no. 115 A

Resultater:

| Nr | ID | F _m kN | S _m N/mm ² | h mm |
|----|-------------|----------------------|-------------------------------------|---------|
| 15 | fly-ash-c-1 | 46,12 | 21,71 | 92,0 |

Grafisk fremstilling:



Statistikk:

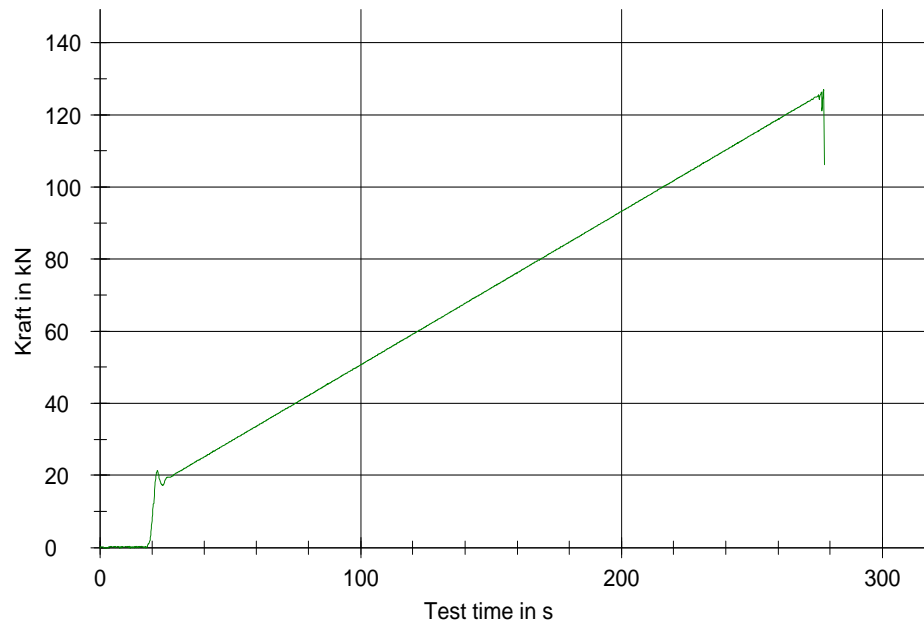
| Series | F _m kN | S _m N/mm ² | h mm |
|-----------|----------------------|-------------------------------------|---------|
| n = 1 | | | |
| \bar{x} | 46,12 | 21,71 | 92,0 |
| s | - | - | - |
| n | - | - | - |

Figure B.1: Results and graph for sample 115 A from the UCS test. The graph shows the applied force (kN) on the y-axis and the time (sec) on the x-axis.

Resultater:

| Nr | ID | F _m kN | S _m N/mm ² | h mm |
|----|-------------|----------------------|-------------------------------------|---------|
| 18 | fly-ash-c-2 | 126,97 | 59,79 | 89,0 |

Grafisk fremstilling:



Statistikk:

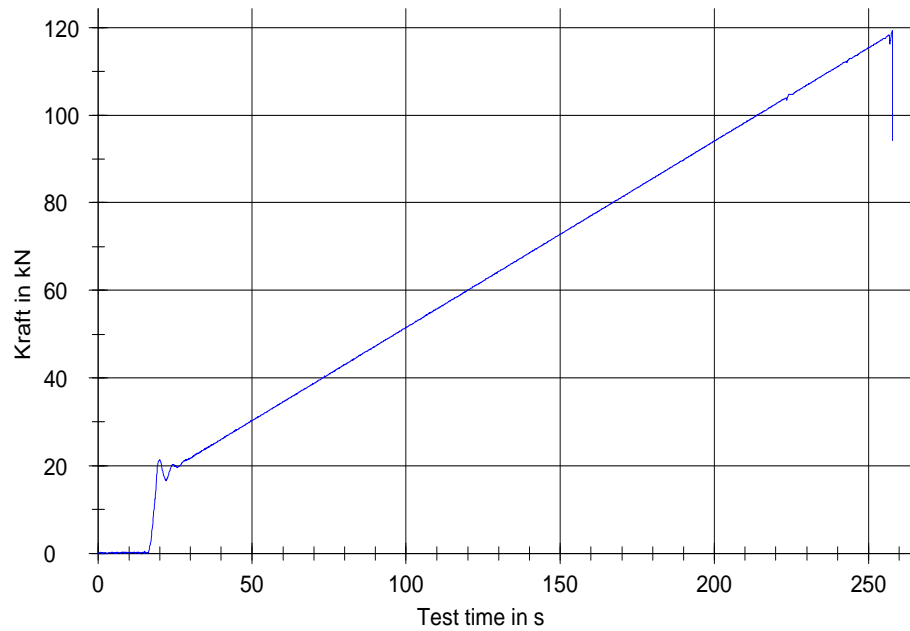
| Series n = 1 | F _m kN | S _m N/mm ² | h mm |
|-----------------|----------------------|-------------------------------------|---------|
| x | 126,97 | 59,79 | 89,0 |
| s | - | - | - |
| n | - | - | - |

Figure B.2: Results and graph for sample 115 B from the UCS test. The graph shows the applied force (kN) on the y-axis and the time (sec) on the x-axis.

Resultater:

| Nr | ID | F _m kN | S _m N/mm ² | h mm |
|----|-------------|----------------------|-------------------------------------|---------|
| 19 | fly-ash-c-3 | 119,29 | 56,17 | 87,0 |

Grafisk fremstilling:



Statistikk:

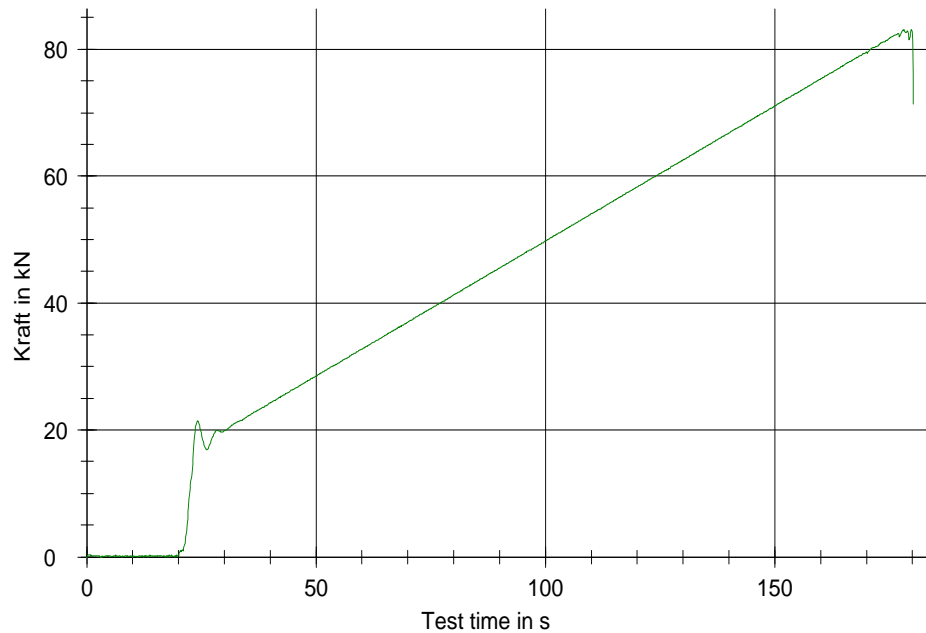
| Series | F _m kN | S _m N/mm ² | h mm |
|-----------|----------------------|-------------------------------------|---------|
| n = 1 | | | |
| \bar{x} | 119,29 | 56,17 | 87,0 |
| s | - | - | - |
| n | - | - | - |

Figure B.3: Results and graph for sample 115 C from the UCS test. The graph shows the applied force (kN) on the y-axis and the time (sec) on the x-axis.

Resultater:

| Nr | ID | F _m kN | S _m N/mm ² | h mm |
|----|-----|----------------------|-------------------------------------|---------|
| 31 | 131 | 83,14 | 39,15 | 87,0 |

Grafisk fremstilling:



Statistikk:

| Series n = 1 | F _m kN | S _m N/mm ² | h mm |
|-----------------|----------------------|-------------------------------------|---------|
| \bar{x} | 83,14 | 39,15 | 87,0 |
| s | - | - | - |
| n | - | - | - |

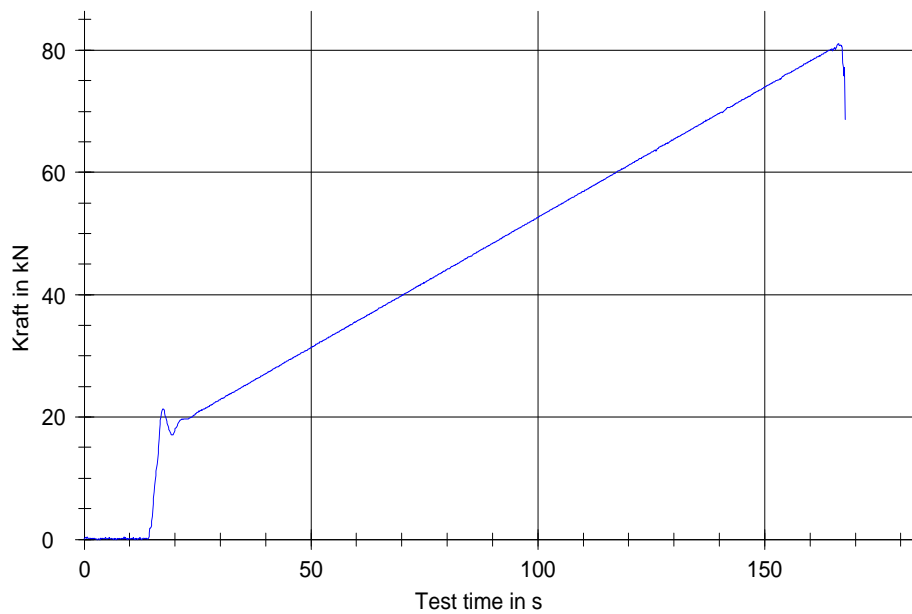
Figure B.4: Results and graph for sample 131 A from the UCS test. The graph shows the applied force (kN) on the y-axis and the time (sec) on the x-axis.



Resultater:

| Nr | ID | F _m kN | S _m N/mm ² | h mm |
|----|------|----------------------|-------------------------------------|---------|
| 32 | 131b | 81,10 | 38,19 | 87,0 |

Grafisk fremstilling:



Statistikk:

| Series | F _m kN | S _m N/mm ² | h mm |
|-----------|----------------------|-------------------------------------|---------|
| n = 1 | | | |
| \bar{x} | 81,10 | 38,19 | 87,0 |
| s | - | - | - |
| n | - | - | - |

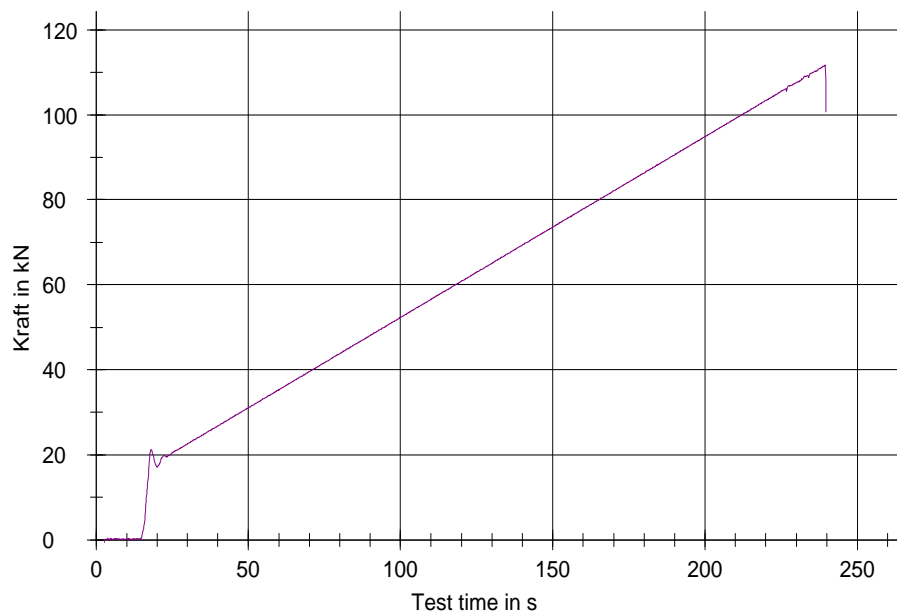
Figure B.5: Results and graph for sample 131 B from the UCS test. The graph shows the applied force (kN) on the y-axis and the time (sec) on the x-axis.



Resultater:

| Nr | ID | F _m kN | S _m N/mm ² | h mm |
|----|-----|----------------------|-------------------------------------|---------|
| 29 | 132 | 111,70 | 52,60 | 87,0 |

Grafisk fremstilling:



Statistikk:

| Series n = 1 | F _m kN | S _m N/mm ² | h mm |
|-----------------|----------------------|-------------------------------------|---------|
| \bar{x} | 111,70 | 52,60 | 87,0 |
| s | - | - | - |
| n | - | - | - |

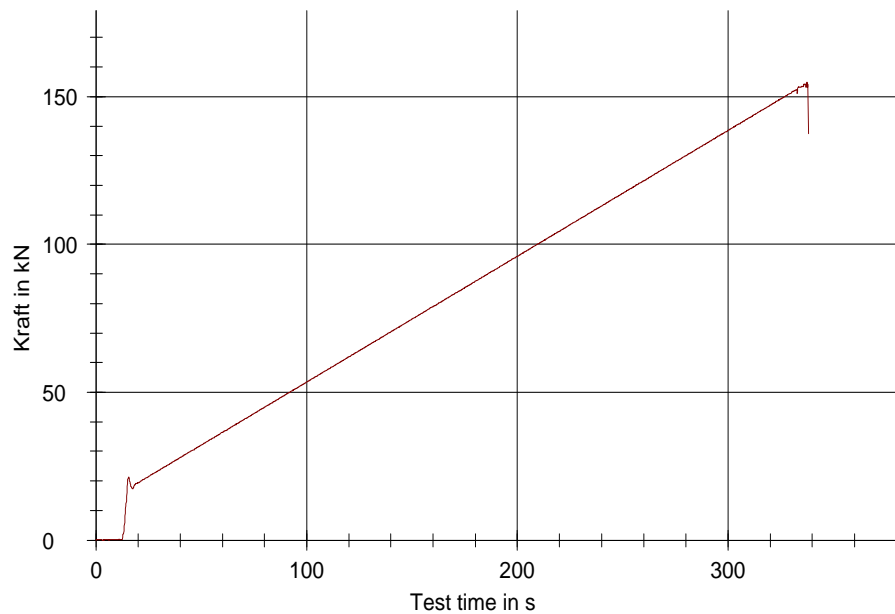
Figure B.6: Results and graph for sample 132 A from the UCS test. The graph shows the applied force (kN) on the y-axis and the time (sec) on the x-axis.



Resultater:

| Nr | ID | F _m kN | S _m N/mm ² | h mm |
|----|------|----------------------|-------------------------------------|---------|
| 30 | 132b | 154,97 | 72,97 | 87,0 |

Grafisk fremstilling:



Statistikk:

| Series | F _m kN | S _m N/mm ² | h mm |
|-----------|----------------------|-------------------------------------|---------|
| n = 1 | | | |
| \bar{x} | 154,97 | 72,97 | 87,0 |
| s | - | - | - |
| n | - | - | - |

Figure B.7: Results and graph for sample 132 B from the UCS test. The graph shows the applied force (kN) on the y-axis and the time (sec) on the x-axis.